



University
of Glasgow

Bishop, P., and Goldrick, G. (2010) *Lithology and the evolution of bedrock rivers in post-orogenic settings: Constraints from the high elevation passive continental margin of SE Australia*. Geological Society, London, Special Publications, 346. pp. 267-287. ISSN 0305-8719

<http://eprints.gla.ac.uk/33314>

Deposited on: 23 February 2012

1 **Lithology and the evolution of bedrock rivers in post-orogenic settings: Constraints from**
2 **the high elevation passive continental margin of SE Australia**

3
4
5 Paul Bishop^{1*} and Geoff Goldrick^{2†}

6
7 School

8 ¹~~Department~~ of Geographical and Earth Sciences, East Quadrangle, University of Glasgow,
9 Glasgow G12 8QQ, UK

10 ²School of Geography and Environmental Science, Monash University, VIC 3168, Australia

11 *e-mail: paul.bishop@ges.gla.ac.uk

12 Corresponding author: Paul Bishop

13 8363 words of text

14 93 References

15 Two Tables

16 Eleven Figures

17 Running header: **Lithology and bedrock rivers in a post-orogenic setting**

18
19 **Abstract**

20 Understanding the role of lithological variation in the evolution of topography remains a
21 fundamental issue, especially in the neglected post-orogenic terrains. Such settings represent
22 the major part of the Earth's surface and recent modelling suggests that a range of interactions
23 can account for the presence of residual topography for hundreds of million years, thereby
24 explaining the great antiquity of landscapes in such settings. Field data from the inland flank of
25 the SE Australian high-elevation continental margin suggest that resistant lithologies act to retard
26 or even preclude the headward transmission of base-level fall driven by the isostatic response to
27 regional denudation. Rejuvenation, be it episodic or continuous, is 'caught up' on these resistant
28 lithologies, meaning in effect that the bedrock channels and hillslopes upstream of these 'stalled'
29 knickpoints have become detached from the base-level changes downstream of the knickpoints.
30 Until these knickpoints are breached, therefore, catchment relief must increase over time, a
31 landscape evolution scenario that has been most notably suggested by Crickmay and Twidale.
32 The role of resistant lithologies indicates that detachment-limited conditions are a key to the
33 longevity of some post-orogenic landscapes, whereas the general importance of transport-limited
34 conditions in the evolution of post-orogenic landscapes remains to be evaluated in field settings.
35 Non-steady-state landscapes may lie at the heart of widespread, slowly evolving post-orogenic
36 settings, such as high-elevation passive continental margins, meaning that non-steady
37 landscapes, with increasing relief through time, are the 'rule' rather than the exception.

† Present address: Coffs Harbour Senior College, Coffs Harbour, NSW 2450, Australia.

38

39

40 Bedrock channels are the 'backbone' of the landscape because they set much of the relief
41 structure of tectonically active landscapes and dictate relationships between relief, elevation and
42 denudation (Howard *et al.* 1994; Whipple & Tucker 1999; Hovius 2000). Bedrock channel
43 evolution is thus the key to understanding landscape history and sediment flux: bedrock trunk
44 channels provide the baselevel to which the whole drainage net and hillslope processes operate
45 (Wohl & Merritt 2001). The last two decades have seen a blossoming of research on bedrock
46 channels, reviving interest in, and building on, the fundamental research of Hack (1957) and Flint
47 (1974) (Tinkler & Wohl 1998). This recent research has addressed a wide range of aspects of
48 bedrock river morphology and processes, including: the distinction between debris-flow bedrock
49 channels and fluvial bedrock channels (e.g., Stock & Dietrich 2003); the stream-power rule for
50 bedrock river incision and its application in the numerical modelling of landscape evolution (e.g.,
51 Howard & Kerby 1983; Howard *et al.* 1994; Whipple & Tucker 1999; Tucker & Whipple 2002; van
52 der Beek & Bishop 2003); refinement of the stream-power rule to take explicit account of
53 sediment (e.g., Sklar & Dietrich 1998, 2001; Turowski *et al.* 2007); bedrock river long profile
54 morphology and development (e.g., Bishop *et al.* 1985; Merritts *et al.* 1994; Whipple *et al.* 2000;
55 Roe *et al.* 2002; Kirby *et al.* 2003; Kobor & Roering 2004; Brocard & van der Beek 2006; Goldrick
56 & Bishop 2007); bedrock river knickpoint processes (Holland & Pickup 1976; Gardner 1983;
57 Hayakawa & Matsukura 2003; Bishop *et al.* 2005; Crosby & Whipple 2006; Frankel *et al.* 2007);
58 and bedrock river incision rates and processes (e.g., Bishop 1985; Burbank *et al.* 1996; Sklar &
59 Dietrich 1998; Hancock *et al.* 1998; Hartshorn *et al.* 2002). The development of cosmogenic
60 nuclide analysis (e.g., Bierman 1994; Bierman & Nichols 2004), with its capability of determining
61 the exposure ages and/or erosion rates of bedrock surfaces, has been a fundamentally important
62 breakthrough in studying bedrock channels (e.g., Burbank *et al.* 1996; Hancock *et al.* 1998;
63 Brocard *et al.* 2003; Reusser *et al.* 2006).

64 Much of this research has had a focus (explicit or implicit) on tectonically active areas,
65 where high rates of rock uplift, high rates of seismicity, and high (to extreme) rates of
66 precipitation 'drive' bedrock incision (e.g., Burbank *et al.* 1996; Hovius 2000; Hartshorn *et al.*
67 2002; Dadson *et al.* 2003, 2004). Likewise, steady-state rivers, in which rock uplift is matched by
68 river incision and/or catchment lowering, underpin numerical modelling of bedrock rivers (e.g.,
69 Whipple & Tucker 1999) and physical modelling of eroding landscapes (e.g., Bonnet & Crave
70 2003). Less attention has been paid in recent work to post-orogenic terrains, such as passive
71 continental margins, that are not experiencing ongoing tectonically-driven rock uplift (Bishop
72 2007). The focus on steady-state tectonically active terrains and the relative neglect of post-
73 orogenic terrains probably reflect the fewer complexities associated with the conceptualisation
74 and numerical modelling of denudation of steady-state terrains (e.g., Whipple & Tucker 1999),

75 and the impressive and eye-catching excitement of tectonically active terrains, where bedrock
76 channel lowering may be physically measured in just one year (e.g., Hartshorn *et al.* 2002). On
77 the other hand, the focus on orogenic belts has drawn attention away from understanding
78 bedrock river processes and long-term landscape evolution in non-orogenic and post-orogenic
79 areas, which constitute by far the majority of the Earth's sub-aerial surface area and which were
80 the focus of research when geomorphology was first emerging as a discipline (Davis 1899,
81 1902).

82 Passive margin highland belts are perhaps the single post-orogenic terrain to have
83 continued to receive widespread attention in the last two decades, especially in terms of low-
84 temperature thermochronology (Moore *et al.* 1986; Dumitru *et al.* 1991; Brown *et al.* 2000a,
85 2000b; Persano *et al.* 2002, 2005), landscape evolution (e.g., Bishop 1985, 1986; Gilchrist &
86 Summerfield 1990; Pazzaglia & Gardner 1994, 2000; Gunnell & Fleitout 1998, 2000; Cockburn *et al.*
87 *et al.* 2002; Matmon *et al.* 2002; Campanile *et al.* 2008), bedrock river evolution (e.g., Bishop *et al.*
88 1985; Young & McDougall 1993; Goldrick & Bishop 1995), and numerical modelling (e.g., Kooi &
89 Beaumont 1994; Tucker & Slingerland 1994; van der Beek & Braun 1998; van der Beek *et al.*
90 1999, 2001). Baldwin *et al.* (2003) used numerical modelling to explore the factors responsible
91 for landscape persistence and the timescales of post-orogenic decay of topography. Their work
92 addresses the formerly-widespread viewpoint that landscapes cannot be much older than the
93 Tertiary and are probably no older than the Pleistocene (e.g., Thornbury 1969), a viewpoint
94 which is demonstrably incorrect in many post-orogenic terrains (Young 1983; Twidale 1998).
95 Baldwin *et al.* (2003) showed that a 'standard' detachment-limited river incision numerical model
96 predicts that orogenic topography will decay to 1% of the original topography at the channel head
97 within only about 1-10 Myr of the cessation of orogenic activity. The addition of isostatic
98 compensation (i.e., rock uplift in response to denudation) increases the decay time to 10-30 Myr,
99 and a switch to transport-limited conditions extends this to 36-90 Myr. Finally, if a critical shear
100 stress for erosion is introduced, along with stochastic variability of flood discharge, the timescale
101 of post-orogenic decay of topography extends to hundreds of millions of years.

102 Baldwin *et al.* (2003) also identified, but did not assess, other factors that could control
103 the rate of post-orogenic topographic decay, including the slowing of landscape evolution by
104 resistant lithologies. In this mechanism, resistant lithologies control the relaxation time of the
105 long profile in (re-)attaining some form of equilibrium (steady-state) long profile after perturbation.
106 We focus on this issue here and ask the question: What role does lithology play in bedrock river
107 morphology and landscape evolution in post-orogenic terrains? We examine this issue in the
108 context of the post-orogenic setting of the Lachlan River catchment on the high elevation passive
109 continental of southeastern Australia, by analysing the long profile morphology of the right- and
110 left-bank tributaries of the upper Lachlan River, one of the major streams that drains the inland

111 flank of the SE Australian highlands. Our long profile analysis is based on the DS form of the
 112 equilibrium bedrock river long profile (Goldrick & Bishop 2007).

113

114 **Background: DS plots and long profile analysis and projection**

115

116 The DS form of the equilibrium long profile plots the logarithm of a reach's slope against the
 117 logarithm of that reach's downstream distance; it is a slope-distance equivalent (hence 'DS') of
 118 the slope-area plot (e.g., Whipple & Tucker 1999) and takes the following form (Goldrick &
 119 Bishop 2007):

$$120 \quad S = kL^{-\lambda} \quad \text{or} \quad \ln S = \gamma - \lambda \ln L \quad 1$$

121 where S is channel slope, L is downstream distance, λ is a constant, k is a constant equal to

122 $\frac{RI_{grade}}{il}$, and γ is equal to $\ln k$. R is some measure of lithological resistance to erosion, I_{grade} is

123 the equilibrium rate of channel incision, i is a constant that describes the proportion of stream

124 power that is expended in incision, and l is a constant.

125 A key feature of the DS form of the long profile is that, in principle, transient channel
 126 steepening, such as a knickpoint propagating in response to base-level fall, can be distinguished
 127 from equilibrium channel steepening in response to a more resistant lithology. The latter
 128 (equilibrium steepening on more resistant lithology) is indicated on the DS plot by a parallel shift
 129 in the plot, whereas a disequilibrium knickpoint plots as disordered outliers on the DS plot
 130 (Goldrick & Bishop 2007).

131 Long-profile disequilibrium is commonly generated by a drop in base-level and is resolved
 132 over time by the upstream passage of a wave of incision (a knickpoint), either as a retreating
 133 step that maintains the knickpoint's height and form, or as a step that rotate backwards by
 134 'inclination' or 'replacement' and diffuses away (Gardner 1983; Bishop *et al.* 2005; Crosby &
 135 Whipple 2006; Frankel *et al.* 2007). At any time between the initiation of a persistent, retreating
 136 knickpoint and its arrival at the stream's headwaters the stream can be thought of as consisting
 137 of three reaches: the upstream reach, which is yet to be affected by the rejuvenation and may
 138 therefore remain graded to the previous base-level; the over-steepened reach comprising the
 139 knickpoint; and the downstream reach that is graded to the new base-level. In order to compare
 140 present and past base-levels (and thereby to quantify, for example, the amount of trunk stream
 141 incision as a result of base-level driven by surface uplift), it is necessary to reconstruct the pre-
 142 rejuvenation profile using the upstream (unrejuvenated) reach and to project that reconstructed
 143 profile downstream.

144 With the exception of theory-free curve fitting (e.g. Jones 1924; Hovius 2000), long profile
 145 reconstructions and projections used to compare present and ancient profiles and to identify

146 changes in base-level have been based on *a priori* models of the equilibrium long profile. We
 147 here use the DS form for such projections, re-arranging Goldrick & Bishop's (2007) equation 2 to
 148 yield:

$$149 \quad \ln(H_0 - H) = \ln\left(\frac{k}{1-\lambda}\right) + (1-\lambda)\ln L \quad 2$$

150 It follows from equation 2 that the value of λ can be determined from the slope of a least-squares
 151 linear regression of the log of downstream distance versus the log of the fall ($H_0 - H$). Once the
 152 value of λ has been determined, the value of k can be determined from the intercept (b) of the
 153 same regression:

$$154 \quad b = \ln\frac{k}{1-\lambda} \quad \text{or} \quad k = (1-\lambda)e^b \quad 3$$

155 The difficulty in solving for λ and k comes from the need to know the value of H_0 , which is not the
 156 same as the elevation of the divide (Goldrick & Bishop 2007). This difficulty can be overcome by
 157 solving equations 2 and 3 iteratively. Estimates of H_0 can be substituted into equation 2 to yield
 158 values of λ which are used in turn to derive values of k . These can then be substituted into
 159 equation 2 to give a mathematical description of the long profile. The goodness of fit of each
 160 description so generated can be evaluated by comparison with the observed profile using the
 161 criterion of the standard error of the estimate of elevation, se_H (Goldrick & Bishop 2007). This
 162 procedure is repeated and the best estimate of H_0 determined by converging on that value which
 163 yields the best fit between the modelled and observed long profile.

164 The downstream projection of the equilibrium reach above a knickpoint to estimate the
 165 amount of base-level fall is illustrated by a hypothetical example in Fig. 1, which shows a stream
 166 with a knickpoint at A and a profile reconstruction and projection based on the DS model of the
 167 graded reach upstream of A. The magnitude of the 40 m base-level fall that generated the
 168 knickpoint at A can be estimated by projecting the reconstructed equilibrium profile above A to
 169 the stream's base-level (Goldrick & Bishop 1995, 2007). The difference between the elevation
 170 predicted by the reconstructed profile and the actual elevation at any point along the stream is
 171 here called H^* , and the value of this difference at base-level at the downstream limit of the
 172 stream is designated H^*_D . H^*_D is an estimate of the magnitude of stream incision in response to
 173 the base-level fall. The DS model prediction of the amount of incision/base-level fall at the
 174 downstream limit of the channel in Fig. 1 is 35 m whereas the 'true' value is 40 m. The
 175 discrepancy of 5 m between the actual base-level drop and the value of H^*_D given by the DS
 176 model is mainly a result of the variability resulting from the standard error of 2 m associated with
 177 the elevation data. In consequence the calculated values of λ and k are 0.89 and 48,
 178 respectively, rather than the "true" values of 0.9 and 50.

179 The confidence interval for H^*_D is given by:

$$t \sqrt{\frac{\sum_{j=1}^n (H_j - \hat{H}_j)^2}{n-2} \left(\frac{1}{n} + \frac{(L_j - \bar{L})^2}{\sum_{j=1}^n L_j^2 - n\bar{L}^2} \right)} \quad 4$$

180
181 where j is the point for which the confidence interval is to be calculated; n is the total number of
182 points; H_j and \hat{H}_j are the observed and predicted elevations at j , respectively; L_j is the
183 downstream distance of j ; and, \bar{L} is the mean value of L (after Ebdon 1985 p.117). A 95%
184 confidence interval for the example in the preceding paragraph gives $H_D^* = 34 \pm 7$ m, a range
185 which encompasses the actual base-level drop of 40 m. This range is large, relative to the size
186 of the base-level drop, an outcome that emphasises the sensitivity of long profile projections to
187 errors in the input data, especially when a projection is made over long distances.

188 The projection of reconstructed profiles to the downstream limit of the stream enables the
189 estimation of total base-level fall to which the stream has responded by incision and knickpoint
190 propagation. Profile projection can also be used to quantify the height of a knickpoint, for which
191 a projection is made from the (graded) section above the knickpoint to the upstream limit of the
192 (graded) section downstream of the knickpoint. In the case of the stream in Fig. 1, projection to
193 the upstream limit of the graded reach below A estimates the height of the knickpoint to be $41 \pm$
194 2 m.

195

196 **Denudational isostatic rebound of the Lachlan catchment and long profile adjustment**

197

198 The Lachlan River catchment drains the inland (western) side of Australia's southeastern
199 Highlands on the Tasman passive continental margin (Fig. 2). The Lachlan is bounded to the
200 east by the continental divide, to the west by the Cenozoic intracratonic Murray Basin, and to the
201 north and the south by catchments of the Macquarie and Murrumbidgee Rivers, respectively.
202 Downstream of Mandagery Creek, the Lachlan flows across a low gradient interior depositional
203 lowlands before terminating in a very low gradient inland swamp (O'Brien & Burne 1994). The
204 Murray-Darling system has its base level in the Southern Ocean some 1000 km downstream of
205 Mandagery Creek, the downstream limit of the study area here (Fig. 2). The distance across the
206 low gradient, swampy, depositional lowlands to the base-level in the Southern Ocean means that
207 Cenozoic eustatic sea-level fluctuations are unlikely to have rejuvenated the Lachlan long profile.

208 Basaltic lavas were erupted into the Lachlan catchment at various times in the Tertiary,
209 providing data on the drainage net at the times of eruption (Bishop *et al.* 1985; Bishop 1986). K-
210 Ar ages on the basalts, coupled with reconstructions of the valleys into which the basalts flowed,
211 demonstrate that much of the relief and many of the drainage systems of the SE Highlands,
212 including the drainage network of the Lachlan, were established by the Early to Middle Tertiary

213 (Wellman & McDougall 1974; Bishop *et al.* 1985; Bishop 1986; Young & McDougall 1993). These
 214 data notwithstanding, the history of the SE Highlands in New South Wales remains somewhat
 215 controversial in detail (Bishop & Goldrick 2000). It has been widely accepted that highlands
 216 surface uplift was related to Tasman margin extension and rifting around 100-90 Ma (Veevers
 217 1984; Wellman 1987; Ollier & Pain 1994; O'Sullivan *et al.* 1995, 1996), which may have
 218 'rejuvenated' a pre-existing topography (e.g., Persano *et al.* 2005). Few find evidence for active
 219 Neogene uplift of this portion of the highlands, notable exceptions being Wellman (1979a 1987),
 220 van der Beek *et al.* (1995) (but see van der Beek *et al.*, 1999), and Tomkins & Hesse (2004) for
 221 the catchment to the north. Recent interpretations of widespread neotectonics in Australia (see
 222 Quigley *et al.* this volume) do not seem relevant to the Lachlan, however, where the known rates
 223 of catchment-wide Neogene denudation of the Lachlan (Bishop 1985) and the isostatic
 224 equilibrium of the highlands (Wellman 1979b) mean that denudational isostasy can account for
 225 the observed Neogene rock uplift in the Lachlan (Bishop & Brown 1992, 1993).

226 The strongest evidence for, and constraint upon, rock uplift along the Lachlan's highlands
 227 margin, whatever the mechanism for that uplift is, comes from the 12 Myr old Boorowa basalt
 228 (informal name), at the inland edge of the highlands (van der Beek & Bishop 2003) (Figs 2 and
 229 3). This basalt overlies fluvial gravels at an elevation 65 m above the modern Lachlan River,
 230 indicating a long-term incision rate of about 5 m Ma⁻¹. This incision must approximate the
 231 amount of relative base-level fall at the highlands margin, which forms base-level for the bedrock
 232 Lachlan catchment studied here. In the absence of relative base-level fall at the highlands
 233 margin, incision rates at the highlands margin should be close to zero. Indeed, where the base-
 234 level is the margin between an eroding highlands and a depositional basin, as it is in the case of
 235 the Lachlan, one might expect an absence of surface uplift to be accompanied by aggradation of
 236 the base level and a gradual up-catchment shift in the margin by back-filling of the highlands
 237 valley. In fact, the Lachlan upstream of the Boorowa basalt is characterised by an incised
 238 bedrock gorge with terraces up to 35m above the modern river (Bishop & Brown 1992; van der
 239 Beek & Bishop 2003). As noted above, the known rates of denudation of the Lachlan catchment
 240 (Bishop 1985) mean that such base-level fall is most reasonably interpreted as the result of
 241 isostatic response to catchment-wide denudation (Bishop & Brown 1992, 1993).

242

243

The upper Lachlan

244

245 Bedrock in the Lachlan catchment consists of meridional belts of Palaeozoic granites and quartz-
 246 rich metasediments and silicic volcanics (Fig. 3). The only post-Palaeozoic rocks are the thin
 247 Tertiary basaltic lavas noted above and sediments scattered throughout the catchment and
 248 sporadic patches of Quaternary alluvium along drainage lines. Even in the areas of apparently
 249 more continuous alluvium, the channel bed appears to be everywhere formed in bedrock.

250 Sediment that locally blankets the channel bed reflects catchment disturbance and sediment
 251 mobilisation over the last century or so, following the introduction of sheep farming by European
 252 settlers. Thus, the entire drainage net is essentially formed in bedrock.

253 The narrow flows of Early Miocene Bevendale Basalt and Wheeo Basalt lie adjacent to
 254 the modern streams in the upper Lachlan (Fig. 4) (Bishop 1984). These flows thus provide a
 255 maximum time limit for stream evolution and have been used several times for the study of
 256 evolution of bedrock river long profiles (Bishop *et al.* 1985; Stock & Montgomery 1999; van der
 257 Beek & Bishop 2003) . The flows are thin valley-fill basalts, preserving the ancient valleys into
 258 which they flowed (Fig. 4). Field relationships, such as the uniform elevation of the upper
 259 surfaces of the highest flow remnants, well below the interfluves, and the lack of any basalt
 260 remnants at higher elevations, demonstrate that the lavas did not fill their valleys and overtop the
 261 interfluves (Bishop *et al.* 1985; Bishop 1986). Post-basaltic stream incision has resulted in relief
 262 inversion so that flows now persist as hilltop remnants and ridges that discontinuously preserve
 263 the E Miocene valleys.

264 The basement geology of the upper Lachlan consists of Ordovician quartz-rich slate and
 265 greywacke of the Adaminaby Group surrounding gneissic granites of the Wyangala Batholith
 266 (Fig. 4); all of these lithologies show meridional foliation. A well-defined band of locally high relief
 267 roughly coincides with the western parts of the granite, which is drained by the upper Lachlan's
 268 eastern (right-bank) tributaries, whereas the Ordovician metasediments drained by the lower-
 269 relief western (left-bank) tributaries are associated with lower relief due to their lower resistance
 270 to erosion. A prominent ridge of resistant contact metamorphic hornfels extends for a
 271 considerable length along the western contact of the Ordovician sediments with the granite (Fig.
 272 4). The modern Lachlan Rivers lies a few kilometres to the west of this ridge, with right-bank
 273 tributaries flowing westward from the granite through the ridge; basalt remnants demonstrate that
 274 the same situation pertained in the E Miocene.

275 Goldrick & Bishop's (2007) preliminary DS analysis of the right- and left-bank long
 276 profiles showed that the right-bank steepened reaches on and about the resistant hornfels and
 277 granite lithologies are disequilibria: the DS profiles of the right-bank tributaries exhibit two outliers
 278 associated with the resistant hornfels and the granite, with these DS outliers separating
 279 essentially linear DS reaches that we interpreted to be in equilibrium (graded). The left-bank
 280 tributaries are much less perturbed by disequilibria and generally grade smoothly to the trunk
 281 stream. We now examine this asymmetry further, using the DS plots.

282

283 **The upper Lachlan's right-bank (eastern) tributaries**

284

285 The right-bank tributaries rise at the continental divide, descending the eastern flank of the upper
 286 Lachlan's valley to the Lachlan; in doing so, they cut through the hornfels ridge and across the

287 Bevendale Basalt. The formerly continuous valley-filling basalt thus now crops out as a series of
288 hill-top cappings isolated from each other by the tributaries.

289 We digitised the 'blue lines' on the New South Wales Central Mapping Authority's 1:50,000
290 topographic sheets (20 m contour interval) to generate long profiles and DS plots of the perennial
291 streams of the Lachlan's highlands drainage net (Goldrick & Bishop 2007). As we noted above,
292 the right-bank tributaries generally exhibit linear (equilibrium) DS profiles separated by
293 knickpoints. Streams 59 and 60 are useful exemplars of these long profile characteristics; they
294 are twin lateral streams to the major east-west remnant of the lava that flowed to the trunk
295 Lachlan from the continental divide in the E Miocene (Bishop 1986) (Figs 5 and 6).

296 Stream 59 rises on the Adaminaby Group metasediments and flows westward across the
297 Wyangala Batholith below that east-west basalt cap. It cuts through the hornfels ridge and the
298 line of the basalt before joining the trunk stream. The DS plot shows that, with the exception of a
299 small discontinuity, stream 59 is graded where it flows across the Adaminaby Group sediments
300 (the standard error of the estimate of elevation, $se_H = 1.0$ m). Downstream, on the Wyangala
301 Batholith, the DS plot is marked by high variability and several peaks or knickpoints, including
302 one where the stream crosses the hornfels ridge. The long profile (Fig. 6a) shows that a
303 downstream projection based on the upstream graded reach projects approximately to the base
304 of the basalt where the stream cuts through it. At that point, the projection yields a value of H^*
305 equal to 60 ± 10 m.

306 Stream 60 is almost the mirror image of Stream 59, rising on the Adaminaby Group
307 metasediments and flowing westward across the granite, through the hornfels ridge, between
308 basalt remnants and then joining the trunk Lachlan. The DS plot (Fig. 6b) shows a low-variability
309 upstream reach that appears graded but the value of se_H is high at 2.8 m. Downstream of that
310 graded reach there is high variability in the DS plot including two well defined knickpoints, with
311 the second of those located immediately upstream of the hornfels ridge. These knickpoints are
312 clearly evident on the long profile (Fig. 6b). Downstream projection of the graded reach is graded
313 approximately to the basalt, with a value of H^* equal to 83 ± 13 m where it crosses the line of the
314 basalt.

315 The profiles of all the eastern right-bank tributaries are broadly similar to Streams 59 and 60,
316 being characterised by equilibrium reaches (low variability on the DS plot) interspersed with high-
317 variability disequilibrium reaches. All the profiles show knickpoints near their junction with the
318 trunk stream. The values of H^* associated with these knickpoints are in broad agreement ranging
319 from 60 ± 10 to 83 ± 13 m, save for the anomalously low, and currently inexplicable, $H^* = 16 \pm 4$
320 m for Stream 57 (Table 1a). Streams 57 and 58 also have knickpoints further upstream for
321 which the values of H^* at their confluences with the trunk are 122 and 143 ± 10 m, respectively

322 (no uncertainty is given for the projection of the upstream graded reach in Stream 57 because it
323 is based on only three points) (Table 1b).

324 The spacing of the elevation contours of the base of the basalt shows that the north-south
325 portion paralleling the Lachlan preserves the E Miocene trunk and the east-west portion
326 preserves an E Miocene tributary, with a notably pronounced steepening upstream of the
327 confluence with the trunk (Fig. 4). The sub-basaltic elevation data are sufficiently complete to
328 allow the construction of a DS plot and long profile for the E Miocene channel down which it
329 flowed. This projection assumes that the headwaters of the basalt-filled channel must have been
330 at least as far east as the easternmost outcrop of the valley-filling basalt (asterisk in Fig. 5) and
331 that the headwaters can have been no further east than the modern continental divide, because
332 the position of the continental divide has been stable since pre-Miocene times (Bishop 1986).

333 The Miocene basalt-filled channel's DS plot (Fig. 7) shows a marked terminal knickpoint and
334 a steep, but nonetheless linear reach upstream of that. The best fit for a reconstruction of the
335 long profile based on that linear upstream reach is achieved when the Miocene divide is
336 presumed to be at the eastern limit of the valley-filling basalt (asterisk in Fig. 5), but this is a
337 rather poor fit with se_H equal to 7.5 m. Projecting this profile yields a value of H^* equal to $103 \pm$
338 30 m where the tributary basalt flow meets the Miocene trunk Lachlan at the elbow in the flow
339 adjacent to the modern Lachlan. In short, and notwithstanding the uncertainties, the Miocene
340 tributary, like most of the modern tributaries, was characterised by considerable disequilibrium
341 and a steep fall to the Miocene trunk.

342 The knickpoint steepenings, both modern and Miocene, are broadly spatially associated with
343 granite and/or hornfels, but there is no clear and precise relationship between steepening and
344 geology in general, nor between the terminal knickpoints and the hornfels ridge in particular.
345 Several streams have graded reaches which cross the geological boundaries, while others have
346 knickpoints on both the granite and the metasediments. Only in the case of Stream 59 is the
347 terminal knickpoint coincident with the hornfels ridge. The terminal knickpoints of Streams 60
348 and 58 are upstream of the hornfels ridge on the granite, and the terminal knickpoints of Stream
349 57 and the Miocene tributary are downstream of the hornfels ridge on the metasediments. The
350 clearest relationship that does emerge from the long profiles analysis is that those streams that
351 flow across the path of the Bevendale Basalt have an upstream reach that is graded
352 approximately to the base of the basalt at the point where they cross the basalt.

353

354 **The upper Lachlan's left-bank (western) tributaries**

355

356 Streams 67 and 69 are tributaries of Stream 68 (Fig. 4). The headwaters of Stream 67 flow
357 across granitic rocks of the Wyangala Batholith while downstream reaches flow across
358 metasedimentary rocks of the Adaminaby Group. The headwaters of Stream 68 are also on the

359 granite and in its lower reaches it flows across Adaminaby Group metasediments. Stream 69
 360 flows entirely across metasedimentary rocks of the Adaminaby Group. The long profiles and DS
 361 plots of Streams 67 and 68 (Fig. 8) show that both streams are graded throughout most of their
 362 lengths except for the presence of a relatively small, but well defined, knickpoint on each stream.
 363 The values of H^* at the confluence of Streams 67 and 68 are 30 ± 2 m ($se_H = 0.52$ m) and $25 \pm$
 364 14 m ($se_H = 1.16$ m), respectively. Despite the very large confidence interval associated with the
 365 projection of Stream 68, due to the long distance over which it has been projected, the values of
 366 H^* are very similar suggesting that the knickpoints are the result of base level change rather than
 367 lithological variation (cf. Goldrick & Bishop 1995, 2007). The value of H^* for Stream 68 upstream
 368 of the junction with the Lachlan is 26 ± 17 m, about 50 m less than typical values for the eastern
 369 tributaries, and the projected profile lies approximately 40 m below the basalt.

370 The DS plot of Stream 69 shows that the stream is not far from graded ($se_H = 2.6$ m) but
 371 there is a suggestion of a discontinuity which does not appear to be associated with a lithological
 372 change (Fig. 9a). A projection of the upstream reach of Stream 69 ($se_H = 1.27$ m) to the
 373 confluence with Stream 68 returns a value of $H^* = 16 \pm 5$ m (Fig. 9a). This is similar to the value
 374 of H^* for Stream 68 itself at this point (25 ± 14 m) so that there is a suggestion that the
 375 discontinuity along Stream 69 has a similar baselevel-fall origin to the knickpoints on Streams 67
 376 and 68, but the steepening on the Stream 69 is more a diffuse 'knickzone' than a discrete
 377 knickpoint.

378 In summary: the western tributaries of the upper Lachlan River show some evidence of
 379 disequilibrium steepening unrelated to lithology, but the degree of steepening along these
 380 streams and the corresponding values of H^* (Table 2) are much less than those in the eastern
 381 (right-bank) tributaries. Several of the tributaries have comparable values of H^* at their junctions
 382 lending support to the proposal that this steepening is due to a relative fall in base level.

383

384

Synthesis

385

386 The eastern (right-bank) tributaries are characterised by marked steepening, especially in their
 387 distal reaches, whereas the western (left-bank) tributaries have much smoother profiles. The
 388 southern tributaries are not treated in detail here, but they are transitional between these two
 389 groups with Streams 61 to 63 similar in form to the eastern tributaries and Streams 64 to 66
 390 similar in form to the western tributaries. The obvious and simplest explanation for the
 391 pronounced east-west asymmetry in the tributary long profiles is the lithological influences
 392 exerted on the eastern tributary long profiles by the granite/hornfels combination and the basalt.
 393 The western tributaries flow mainly across Adaminaby Group rocks of moderately low resistance
 394 whereas the eastern tributaries flow across a variety of rock types including the more resistant

395 granites of the Wyangala Batholith and the hornfels ridge. The eastern tributaries also all cut
396 through the Bevendale Basalt upstream of their junctions with the trunk stream. Finally, and
397 most importantly, all the eastern tributaries have a reach that is graded approximately to the
398 base of the Bevendale Basalt where the tributaries cross the line of the basalt.

399 A major perturbation was introduced into the drainage net by the Bevendale Basalt flowing
400 down the east-west tributary and then northward along the Miocene trunk Lachlan. The fact that
401 all the eastern tributaries have a reach that is graded approximately to the base of the Bevendale
402 Basalt suggests the evolutionary history presented schematically in Fig. 10. After the eruption, a
403 new trunk stream formed on the western edge of the valley basalt so that the western tributaries
404 maintained an unimpeded path to that new trunk whereas the eastern tributaries flowed across
405 the newly emplaced (and resistant) valley basalt to join the trunk.

406 The basalt in the trunk would no doubt have introduced some disequilibrium into the
407 profiles of the western streams (flattening them) but in the absence of resistant rocks it is likely
408 that the new trunk and the western tributaries re-attained equilibrium early after the eruption.
409 Disruption of the eastern tributaries must have been considerably greater. The re-establishment
410 of a graded landscape east of the trunk stream would have been inhibited by the greater
411 resistance of the granite, hornfels and the basalt. The influence of the latter was particularly
412 important, because the eastern tributaries' low gradients across the top of the basalt, relative to
413 the basalt's lithological resistance, would have led to a differential between the rate at which the
414 trunk and its western tributaries were incising and that at which the eastern tributaries were
415 incising into the basalt. If the attainment of grade in detachment-limited, post-orogenic settings,
416 such as this, is a 'bottom-up' process (Bishop 2007) then the basalt would have acted as a local
417 base level with the upstream reaches of the eastern tributaries becoming graded to it.
418 Differential incision rates would have resulted in a steepening of the gradients between the new
419 trunk stream and the basalt (Fig. 10 Post-eruption 2).

420 Over time, the trunk would have continued to incise at a faster rate than the tributaries on,
421 and upstream of, the basalt so that the height differential between the two would have increased
422 as would have the gradients across the basalt. Throughout this stage (Fig. 10 Post-eruption 3),
423 the basalt would have acted as a temporary local base level for the eastern tributaries.
424 Eventually these tributaries would have cut through the basalt removing the temporary base level
425 provided by the basalt and triggering the upstream migration of a knickpoint (Fig. 10 Post-
426 eruption 4). This stage, which represents the present state of the upper Lachlan drainage net, is
427 characterised by a downstream disequilibrium reach and an upstream reach which is graded
428 approximately to the level of the basalt remnant at the time when it was breached (i.e., the base
429 of the flow).

430 This model offers the most likely explanation for the gross morphology of the tributaries of the
431 upper Lachlan catchment with the western tributaries essentially graded to the modern trunk with

432 only minor disequilibrium, and the eastern tributaries characterised by marked downstream
 433 disequilibrium steepening and an upstream reach that is graded approximately to the base of the
 434 basalt. The data confirm that resistant lithologies can act a temporary local base levels and
 435 retard the re-establishment of equilibrium, influencing relaxation times of streams so that
 436 resistant reaches can temporarily isolate upstream reaches from the effects of downstream
 437 perturbations.

438

439

Numerical simulation of the influence of lithology on stream evolution

440

441 This interpretation of the role of the basalt in delaying the headward transmission in the right-
 442 bank tributaries of base-level fall in the trunk was tested using a 1D finite difference stream
 443 evolution simulation based on the DS form, in which the amount of incision at each iteration is
 444 determined by the variables k , λ , L , i and S (see eq. 1 above, and Goldrick & Bishop (2007)).
 445 The modelled long profile consists of 100 reaches: reaches 1 to 72 and 89 to 100 have a
 446 lithological resistance corresponding to $R = 50$, and reaches 73 to 88 have a doubled lithological
 447 resistance of $R = 100$. Each point, x , in the long profile is lowered according to the formula:

448

$$incision = \frac{il}{R} L_x^\lambda \left(\frac{H_x - H_{x+1}}{L_{x+1} - L_x} \right) \quad 2$$

449 where H_x , H_{x+1} , L_x and L_{x+1} are the elevations and downstream distances, respectively of x and
 450 $x+1$. At each iteration the amount of incision is calculated for each reach before the elevations
 451 are adjusted.

452

453

454

455

456

457

458

459

460

461

The development of the profile in the “post-eruption” period is recorded in Fig. 11. Fig. 11a
 and b depict the immediate post-eruption profiles of the tributary, which can be divided into three
 reaches. The reach downstream of the basalt is graded to the trunk stream which acts as a base
 level and this reach continues to incise at the same rate as the trunk, at the long-term denudation
 rate driven by denudational isostatic rebound. The reach flowing across the basalt is in
 disequilibrium because its gradient is low relative to the erosional resistance of the basalt, and it
 therefore incises at a slower rate than the trunk and the downstream reach. The reach upstream
 of the basalt is also no longer in equilibrium because the basalt is acting as a temporary local
 base level that is lowering at a slower rate than the base level to which this reach was previously
 graded.

462

463

464

465

466

After 25000 iterations (Fig. 11c and d), a clear knickpoint, indicated by a peak on the DS plot,
 has formed at the downstream edge of the basalt as a result of the rate differential between
 incision on the country rock and on the basalt. This incision rate differential results in a decrease
 in the gradients immediately upstream of the basalt, as indicated by low values on the DS plot
 and the flattening of the long profile immediately upstream of the basalt. After 50000 iterations

467 the knickpoint has eroded through the downstream edge of the basalt and has become more
468 pronounced (Fig. 11e and f). At the same time gradients upstream have decreased as an
469 increasingly extensive reach has become graded to the upstream edge of the basalt.

470 75000 iterations see an even more pronounced knickpoint and the low gradient reach has
471 become more extensive. This pattern continues until, at 125000 iterations, the stream is at the
472 point of breaching the basalt (Fig. 11i and j). After the basalt has been breached, the knickpoint
473 begins to migrate more rapidly upstream and declines ('lies back') so that the peak on the DS
474 plot is less marked and knickpoint becomes laterally more extensive. That is, the knickpoint
475 evolves from a discrete knickpoint into a more diffuse knick-zone. The form of the stream after
476 150000 iterations (Fig. 11k and l) is similar to the modern forms of the eastern tributaries of the
477 upper Lachlan with an upstream reach graded approximately to the base of the basalt, and a
478 knickpoint between this reach and the trunk stream.

479 The simulation is consistent with the hypothesis that basalt (or any other resistant rock)
480 acting as a temporary local base level can retard the development of the upstream reaches,
481 induce the formation of a knickpoint, and produce the type of profile that is typical of the eastern
482 tributaries.

483

484

Discussion

485

486 The 'engine' for landscape evolution in the post-orogenic setting of the Lachlan River is
487 denudational isostatic rebound: denudational unloading of the uplands, at rates of $\sim 5 \text{ m Myr}^{-1}$
488 (Bishop 1985), triggers the isostatic response of rock uplift, which in turn triggers drainage net
489 rejuvenation at the drainage net's base-level (in this case the inland edge of the highlands,
490 where the Lachlan flows onto the sedimentary fill of the continental interior) (Bishop & Brown
491 1992). For reasons that are not yet fully clear, but which likely reflect discontinuous movement on
492 the highland-edge fault(s) on which the denudational isostatic rebound is accommodated, this
493 rejuvenation is evidently discontinuous. Each denudational isostatic uplift 'event' presumably
494 triggers a steepened reach where the Lachlan leaves the highlands around Cowra, and this
495 steepened reach propagates as a knickpoint, headwards along the trunk stream and
496 progressively through the drainage net. The contrast in the long profiles of the upper Lachlan's
497 eastern (right-bank) and western (left-bank) tributaries shows that resistant lithologies act to slow
498 knickpoint propagation, whereas non-resistant lithologies allow rejuvenation to be readily
499 propagated headwards and for graded (equilibrium) long profiles to be re-established (e.g. Fig.
500 9). There are no indications as to the magnitude of each of these rock uplift events, but if the
501 altitudinal separation of each of the terraces in the bedrock reach upstream of the highlands
502 edge (Bishop & Brown 1992) is indicative of the magnitude of the uplift, then each is very
503 substantial. That said, there may be a climatic component to the generation of these terraces

504 and, in any event, the key issues are the triggering of knickpoints at the highlands edge by rock
505 uplift of unknown magnitude as a result of denudational rebound, the propagation of those
506 knickpoints through the drainage net, and the retardation of these knickpoints by resistant
507 lithologies. The values of H^* in the upper Lachlan right-bank tributaries that flow across resistant
508 lithologies integrate all the rebound events for a given time interval.

509 This lithological retardation of knickpoint propagation is independent of the eruption of
510 basalt into the upper Lachlan's drainage net, as confirmed by the knickpoints in the long profile
511 into which the basalt was extruded 21 Ma (Fig. 7). In other words, in the absence of the basalt,
512 the lithological resistance of the granite and hornfels still acts to retard knickpoint propagation.
513 That conclusion is confirmed by the fact that streams 57 and 58 also have upstream knickpoints
514 for which the graded reaches above the knickpoints have values of H^* of 122 and 143 ± 10 m at
515 their confluences with the trunk (see above). Those graded reaches project to elevations above
516 the basalt and so must pre-date that basalt. As shown above (Fig. 7), projection to the trunk
517 stream of the long profile of the basalt-filled east-west tributary yields $H^* = 103 \pm 30$ m and so the
518 graded reaches with $H^* = 122$ and 143 m in streams 57 and 58 are likely to reflect long profile
519 equilibria prior to 21 Ma, given that they project to a base-level in the trunk that is 20-40 m above
520 that to which the basalt-filled E Miocene tributary long profile projects.

521 The perturbation caused by the basalt in the trunk stream is, in one sense, a special
522 case, but it has general implications in enabling us (i) to use the instantaneous 'injection' of a
523 resistant lithology into the long profile to assess the role of resistant lithologies in retarding
524 knickpoint propagation, and (ii) to place that retardation in a dated time-frame. The basalts have
525 clearly retarded the propagation of post-basaltic rejuvenation into the right-bank tributaries, with
526 the implication that the reaches below the lowermost knickpoint in those right-bank tributaries are
527 still adjusting to post-basaltic rejuvenation (unlike the left-bank tributaries which have long ago
528 accommodated the earlier post-basaltic rejuvenation). That is, H^* in the left-bank tributaries is
529 much less than the 50-80 m of post-basaltic incision along the trunk (which approximates the
530 right-bank H^* values of 60-80 m – Table 1). An important implication of that interpretation is that
531 the left-bank tributaries must be incising at approximately the same rate as the trunk Lachlan
532 whereas the right-bank tributaries must have a range of incision rates along their lengths:
533 between the trunk and the right-bank tributaries' first knickpoint, incision rates must range from
534 the Lachlan's rate in the tributaries' downstream reaches, to (much?) higher rates in the
535 knickpoint reaches, where the delayed rejuvenation is still being accommodated. In the graded
536 reaches of the right-bank tributaries above those downstream-most knickpoints, incision rates
537 are set by the channels' discharges, sediment fluxes and gradients and not by the trunk stream's
538 rate of incision. In each case, the knickpoint in effect disconnects the graded reach and the trunk
539 Lachlan.

540 More generally, the data reported here demonstrate the central role that resistant
541 lithologies play in slowing landscape evolution in post-orogenic settings in which landscape
542 response to rock uplift is via bottom-up processes of headward propagating rejuvenation (cf.
543 Baldwin *et al.* 2003). The knickpoints on resistant lithologies in the Lachlan's eastern (right-
544 bank) tributaries mean that the upper catchments are not lowering at the same rate as the trunk
545 stream and the left-bank tributaries, and that the relief of the catchment must be increasing. This
546 conclusion is confirmed by the fact that the headwaters of the modern streams rise on the E
547 Miocene basalts whereas these modern streams have incised below the basalts (Fig. 4) (Bishop
548 *et al.* 1985). We note that the presence of the basalts demonstrates the reality of increasing
549 relief and places a time-scale on that relief increase, but it is not a pre-requisite for that relief
550 increase.

551 The numerical modelling of Baldwin *et al.* (2003) highlights the role of transport-limited
552 conditions in extending the 'life' of post-orogenic terrains to tens and hundreds of millions of
553 years. Those transport-limited conditions mean that river beds consist of a layer of sediment
554 covering the bedrock of the channel bed, shielding it from erosion (cf. Sklar & Dietrich 1998,
555 2001). In such transport-limited situations, rivers rarely 'interact' with the substrate and, in effect,
556 do not 'feel' lithological variation (e.g. Brocard & van der Beek 2006). We do not envisage that
557 situation to be the case in the upper Lachlan, which is characterised by low to very low rates of
558 denudation and sediment flux (cf. Bishop 1985). The knickpoint reaches are not mantled by
559 sediment and so their low rates of erosion are due to a combination of factors including their
560 lithological resistance and the low rates of sediment flux for abrading the bed. In other words,
561 detachment-limited conditions must also be incorporated, and may be a central element, in
562 explanations of the longevity of post-orogenic terrains.

563 We envisage that the knickpoints are slowed and caught on the steeply dipping hornfels
564 and jointed and foliated granites of the upper Lachlan as has been documented in field and
565 laboratory observations by Frankel *et al.* (2007). In their experiments, a knickpoint on steeply
566 dipping resistant lithologies evolved by a combination of parallel retreat on the knickpoint face
567 and vertical channel incision on the knickpoint 'top' (though it is unclear whether this channel
568 incision on the knickpoint top is the commonly observed draw-down effect on knickpoints – Haviv
569 *et al.* (2006)). Whatever its precise nature, that vertical channel incision must limit the height that
570 knickpoints can attain, and, in any event, knickpoints cannot continue to grow indefinitely
571 because knickpoints of extreme heights will not be stable. The Lachlan data show that
572 knickpoints eventually cut through resistant lithologies and continue their headward propagation.
573 Breaching of the basalts reflects the finite vertical thickness of the basalt (Fig. 10) but the
574 presence of more than one knickpoint in some of the right-bank tributaries (e.g., streams 57 and
575 58), with the graded reaches above the upper knickpoints projecting to elevations above the

576 basalt-filled E Miocene channel, confirms that knickpoints do propagate through the hornfels and
577 into the granites.

578 Bishop *et al.* (1985) and Young & McDougall (1993) observed that the passage of the
579 whole of the Neogene (and almost certainly longer) has not resulted in anything that approaches
580 planation of the post-orogenic landscape of SE Australia. Quite the opposite, the data here show
581 increasing relief, much as hypothesised by Crickmay (1974, 1975) and Twidale (1976, 1991),
582 who has been a major champion of Crickmay's "hypothesis of unequal activity". This hypothesis
583 proposes that fluvial erosional energy is progressively concentrated in large river valley bottoms
584 and that lower erosion rates in the smaller rivers of the upland areas mean that denudation of
585 upland areas slows (cf. Bishop 2009). Incision of major channels mean that they become de-
586 coupled from slopes. That is, relief amplitude must increase as rivers continue to incise and
587 upstream areas erode more slowly (Crickmay 1975; Twidale 1976). Formalising this approach in
588 a model of landscape evolution involving increased and increasing relief amplitude (and going
589 beyond the relative sizes of trunk and tributary streams proposed by Crickmay as the key issue),
590 Twidale (1991) highlighted the role of resistant lithologies, structure and different groundwater
591 conditions throughout a drainage basin as the central factors responsible for increasing relief. As
592 Twidale argued: "water ... is concentrated in and near major channels, for, once a master stream
593 develops, not only surface water but subsurface drainage too gravitates towards it ... [U]plift
594 induces stream incision and water-table lowering, leaving high plains and plateaux perched and
595 dry" (Twidale 1998 p.663). The retardation of knickpoints on resistant lithologies adds a further
596 dimension to that argument, as does the lack of discharge and sediment supply to incise the
597 bedrock channels and these knickpoints.

598

599

Conclusion

600

601 The post-orogenic landscape of SE Australia enables the clarification of several major issues in
602 long-term landscape evolution, not least because of its excellent evidence of landscape evolution
603 as recorded by Cenozoic valley-filling basalts. These basalts provide chronologically rigorous
604 evidence of Cenozoic landscape character, long-profile morphology and rates of landscape
605 evolution, as well as the opportunity to assess responses to the perturbation of a major resistant
606 lithology being introduced into the drainage network. The long profile morphology of the Lachlan
607 River drainage net demonstrates that ongoing rock uplift driven by denudational isostatic
608 rebound is propagated headwards through the drainage net from the inland edge of the bedrock
609 highlands. That rock uplift 'signal' is transmitted more rapidly through those parts of the drainage
610 net formed on less resistant lithologies, such as regionally metamorphosed meta-sandstones
611 and phyllites, and more slowly on more resistant granites and contact metamorphic hornfels. The
612 basalts themselves also retard landscape response to rock uplift, but the slowing of such

613 responses occurs on the granites and contact metamorphic rocks, whether the basalts are
614 present or not.

615 Four general conclusions may be drawn from the study reported here:

- 616 1. Denudational isostatic rebound is an important and fundamental mechanism for
617 prolonging the timescale for the postorogenic decay of topography (Bishop & Brown
618 1992; Baldwin *et al.* 2003).
- 619 2. Resistant lithologies, and the delay that they exert on the transmission of the signal of
620 rock uplift triggered by denudational isostatic rebound, are further important factors in
621 prolonging the timescale of postorogenic decay of topography; this second group of
622 factors has hitherto not been evaluated rigorously.
- 623 3. The role of resistant lithologies indicates that detachment-limited conditions are a key to
624 the longevity of (at least some) post-orogenic landscapes. The general importance of
625 transport-limited conditions, as proposed by Baldwin *et al.* (2003), remains to be
626 evaluated in field settings.
- 627 4. The data demonstrate that the appropriate model for the evolution of landscapes such as
628 that described here is one of spatially unequal activity and increasing relief, as Crickmay
629 (1974 1975) and Twidale (1991) have emphasised.

630 The delays in the propagation of knickpoints may persist for considerable periods, reinforced
631 by very low stream power that reflects low discharges in these often semi-arid, intra-continental
632 interiors and their low gradients, as well as low fluxes of sediment to act as erosional 'tools'. In
633 other words, non-steady-state landscapes may lie at the heart of widespread, slowly evolving
634 post-orogenic settings, such as high-elevation passive continental margins, meaning that non-
635 steady landscapes, with increasing relief through time, are the 'rule' rather than the exception on
636 the Earth's surface.

637

638

Acknowledgements

639 This research was supported by a Monash University Graduate Scholarship and a Research and
640 Travel Grant from the University of Edinburgh Department of Geography (both to GG), Australian
641 Research Council grants and a Leverhulme Visiting Fellowship in the University of Edinburgh
642 Department of Geography (both to PB), and Monash University. We thank Peter van der Beek
643 and Colin Pain for their comments which improved the first draft of this chapter. The work
644 reported here is drawn from the PhD theses of the two authors, Bishop's supervised by Martin
645 A.J. Williams and Goldrick's by Bishop. PB records here his sincere thanks to MAJW for
646 inspiration and guidance over an extended period, starting in PB's undergraduate years.
647 Martin's contribution lives on in his students and in their students.

648

649

References

650

- 651 Baldwin, J. A., Whipple, K. X. & Tucker, G. E. 2003. Implications of the shear stress river incision
652 model for the timescale of postorogenic decay of topography. *Journal of Geophysical*
653 *Research*, **108**, B3, 2158, doi:10.1029/2001JB000550.
- 654 Bierman, P. R. 1994. Using in situ produced cosmogenic isotopes to estimate rates of landscape
655 evolution; a review from the geomorphic perspective. *Journal of Geophysical Research*, **99**,
656 13885–13896.
- 657 Bierman, P. R. & Nichols, K. K. 2004. Rock to sediment—slope to sea with ¹⁰Be—rates of
658 landscape change. *Annual Review of Earth and Planetary Science*, **32**, 215–255.
- 659 Bishop, P. 1984. Oligocene and Miocene volcanic rocks and quartzose sediments of the Southern
660 Tablelands, New South Wales: Definition of stratigraphic units. *Journal and Proceedings of the*
661 *Royal Society of N.S.W.*, **117**, 113-117.
- 662 Bishop, P. 1985. Southeast Australian late Mesozoic and Cenozoic denudation rates: A test for late
663 Tertiary increases in continental denudation. *Geology*, **13**, 479-482.
- 664 Bishop, P. 1986. Horizontal stability of the Australian continental drainage divide in south central
665 New South Wales during the Cainozoic. *Australian Journal of Earth Sciences*, **33**, 295-307.
- 666 Bishop, P. 2007. Long-term landscape evolution: Linking tectonics and surface processes. *Earth*
667 *Surface Processes and Landforms*, **32**, 329-365.
- 668 Bishop, P. 2009. Landscape Evolution. In: Gomez, B., Baker, V. R., Goudie, A. S. & Roy, A. G.
669 (eds) *Handbook of Geomorphology*. SAGE Publications, London, In press.
- 670 Bishop, P. & Brown, R. 1992. Denudational isostatic rebound of intraplate highlands: The
671 Lachlan River valley, Australia. *Earth Surface Processes and Landforms*, **17**, 345-360.
- 672 Bishop, P. & Brown, R. 1993. Denudational isostatic rebound of intraplate highlands: The Lachlan
673 River valley, Australia. Reply. *Earth Surface Processes and Landforms*, **18**, 753-755.
- 674 Bishop, P. & Goldrick, G. 2000. Geomorphological evolution of the East Australian continental
675 margin. In: Summerfield, M. A. (ed.) *Geomorphology and Global Tectonics*. John Wiley,
676 Chichester, 227-255.
- 677 Bishop, P., Hoey, T. B., Jansen, J. D. & Artza, I. L. 2005. Knickpoint recession rates and
678 catchment area: The case of uplifted rivers in E Scotland. *Earth Surface Processes and*
679 *Landforms*, **30**, 767–778.
- 680 Bishop, P., Young, R. W. & McDougall, I. 1985. Stream profile change and long-term landscape
681 evolution: Early Miocene and modern rivers of the east Australian highland crest, central New
682 South Wales. *Journal of Geology*, **93**, 455-474.

- 683 Bonnet, S. & Crave, A. 2003. Landscape response to climate change: Insights from experimental
684 modeling and implications for tectonic versus climatic uplift of topography. *Geology*, **31**, 123-
685 126.
- 686 Brocard, G. Y., van der Beek P. A., Bourlès, D. L., Siame, L. L. & Mugnier, J.-L. 2003. Long-term
687 fluvial incision rates and postglacial river relaxation time in the French Western Alps from
688 ¹⁰Be dating of alluvial terraces with assessment of inheritance, soil development and wind
689 ablation effects. *Earth and Planetary Science Letters*, **209**, 197-214, doi: 10.1016/S0012-
690 821X(03)00031-1.
- 691 Brocard, G. Y. & van der Beek, P. A. 2006. Influence of incision rate, rock strength, and bedload
692 supply on bedrock river gradients and valley-flat widths: Field-based evidence and
693 calibrations from western Alpine rivers (southeast France). In: Willett, S. D., Hovius, N.,
694 Brandon, M. T. & Fisher, D. (eds) *Tectonics, Climate, and Landscape Evolution*. Geological
695 Society of America Special Paper, **398**, 101–126, doi: 10.1130/2006.2398(07).
- 696 Brown, R. W., Gallagher, K., Gleadow, A. J. W. & Summerfield, M. A. 2000a. Morphotectonic
697 evolution of the South Atlantic margins of Africa and South America. In: Summerfield, M. A.
698 (ed.) *Geomorphology and Global Tectonics*. John Wiley, Chichester, 255-281.
- 699 Brown, R. W., Summerfield, M. A. & Gleadow, A. J. W. 2000b. Denudational history along a
700 transect across the Drakensberg Escarpment of southern Africa derived from apatite fission
701 track thermochronology. *Journal of Geophysical Research*, **107**, 2350, doi:
702 10.1029/2001JB000745.
- 703 Burbank, D. W., Leland, J., Fielding, E., Anderson, R. S., Brozovic, N., Reid, M. R. & Duncan, C.
704 1996. Bedrock incision, rock uplift and threshold hillslopes in the northwestern Himalayas.
705 *Nature*, **379**, 505-510.
- 706 Campanile, D., Nambiar, C. G., Bishop, P., Widdowson, M. & Brown, R. 2008. Sedimentation
707 record in the Konkan-Kerala basin: Implications for the evolution of the Western Ghats and
708 the Western Indian passive margin. *Basin Research*, **20**, 3–22, doi: 10.1111/j.1365-
709 2117.2007.00341.x.
- 710 Cockburn, H. A. P., Brown, R. W., Summerfield, M. A. & Seidl, M. A. 2002. Quantifying passive
711 margin denudation and landscape development using a combined fission-track
712 thermochronology and cosmogenic isotope analysis approach. *Earth and Planetary Science
713 Letters*, **179**, 429-435.
- 714 Crickmay, C. H. 1974. *The Work of the River*. Macmillan, London.
- 715 Crickmay, C. H. 1975. The hypothesis of unequal activity. In: Melhorn, W. M. & Flemal, R. C.
716 (eds) *Theories of Landform Development*. Publications in Geomorphology, Binghamton,
717 State University of New York, 103-109.
- 718 Crosby, B. T. & Whipple, K. X. 2006. Knickpoint initiation and distribution within fluvial networks:
719 236 waterfalls in the Waipaoa River, North Island, New Zealand. *Geomorphology*, **82**, 16–38.

- 720 Dadson, S. J., Hovius, N., Chen, H., Dade, W. B., Hsieh, M-L., Willett, S. D., Hu, J-C., Horng, M-J.,
721 Chen, M-C., Stark, C., Lague, D. & Lin, J-C. 2003. Links between erosion, runoff variability and
722 seismicity in the Taiwan orogen. *Nature*, **426**, 648-651.
- 723 Dadson, S. J., Hovius, N., Chen, H., Dade, W. B., Lin, J-C., Hsu, M-L., Lin, C-W., Horng, M. J.,
724 Chen, T-C., Milliman, J. & Stark, C. P. 2004. Earthquake-triggered increase in sediment
725 delivery from an active mountain belt. *Geology*, **32**, 733-736.
- 726 Davis, W. M. 1899. The Geographical Cycle. *Geographical Journal*, **14**, 481-504.
- 727 Davis, W. M. 1902. Base-level, grade and the peneplain. *Journal of Geology*, **10**, 77-111.
- 728 Dumitru, T. A., Hill, K. C., Coyle, D. A., Duddy, I. R., Foster, D. A., Gleadow, A. J. W., Green, P. F.,
729 Kohn, B. P., Laslett, G. M. & O'Sullivan, A. J. 1991. Fission track thermochronology: application
730 to continental rifting of south-eastern Australia. *APEA Journal*, **31**, 131-142.
- 731 Ebdon, D. 1985. *Statistics in Geography*. Basil Blackwell, Oxford.
- 732 Flint, J. J. 1974. Stream gradient as a function of order, magnitude and discharge. *Water*
733 *Resources Research*, **10**, 969-973.
- 734 Frankel, K. L., Pazzaglia, F. J. & Vaughn, J. D. 2007. Knickpoint evolution in a vertically bedded
735 substrate, upstream-dipping terraces, and Atlantic slope bedrock channels. *Geological*
736 *Society of America Bulletin*, **119**, 476-486, doi: 10.1130/B25965.1
- 737 Gardner, T. W. 1983. Experimental study of knickpoint and longitudinal profile evolution in
738 cohesive, homogenous material. *Geological Society of America Bulletin*, **94**, 664-667.
- 739 Gilchrist, A. R. & Summerfield, M. A. 1990. Differential denudation and flexural isostasy in
740 formation of rifted-margin upwarps. *Nature*, **346**, 739-742.
- 741 Goldrick, G. & Bishop, P. 1995. Differentiating the roles of lithology and uplift in the steepening of
742 bedrock river long profiles: An example from southeastern Australia. *Journal of Geology*, **103**,
743 227-221.
- 744 Goldrick, G. & Bishop, P. 2007. Regional analysis of bedrock stream long profiles: Evaluation of
745 Hack's SL form, and formulation and assessment of an alternative (the DS form). *Earth*
746 *Surface Processes and Landforms*, **32**, 649-671.
- 747 Gunnell, Y. & Fleitout, L. 1998. Shoulder uplift of the Western Ghats passive margin, India – a
748 flexural model. *Earth Surface Processes and Landforms*, **23**, 135-153.
- 749 Gunnell Y. & Fleitout, L. 2000. Morphotectonic evolution of the Western Ghats, India. *In*:
750 Summerfield, M. A. (ed.) *Geomorphology and Global Tectonics*. John Wiley, Chichester, 320-
751 368.
- 752 Hack, J. T. 1957. Studies of longitudinal stream profiles in Virginia and Maryland. *U.S.*
753 *Geological Survey Professional Paper*, **294-B**, 45-97.
- 754 Hancock, G. S., Anderson, R. S. & Whipple, K. X. 1998. Beyond power: Bedrock River Incision
755 Process and Form. *In*: Tinkler, K. J. & Wohl, E. E. (eds) *Rivers over Rock: Fluvial Processes*
756 *in Bedrock Channels*. American Geophysical Union, Geophysical Monograph, **107**, 35-60.

- 757 Hartshorn, K., Hovius, N., Dade, W. B. & Slingerland, R. L. 2002. Climate-drive bedrock incision
758 in an active mountain belt. *Science*, **297**, 2036-2038.
- 759 Haviv, I., Enzel, Y., Whipple, K. X., Zilberman, E., Stone, J., Matmon, A. & Fifield, L. K. 2006.
760 Amplified erosion above waterfalls and oversteepened bedrock reaches. *Journal of*
761 *Geophysical Research*, **111**, F04004, doi:10.1029/2006JF000461.
- 762 Hayakawa, Y. & Matsukura, Y. 2003. Recession rates of waterfalls in Boso Peninsula, Japan,
763 and a predictive equation. *Earth Surface Processes and Landforms*, **28**, 675-684.
- 764 Holland, W. N. & Pickup, G. 1976. Flume study of knickpoint development in stratified sediment.
765 *Geological Society of America Bulletin*, **87**, 76-82.
- 766 Hovius, N. 2000. Macroscale process systems of mountain belt erosion. *In*: Summerfield, M. A.
767 (ed.) *Geomorphology and Global Tectonics*. John Wiley, Chichester, 77-105.
- 768 Howard, A. D. & Kerby, G. 1983. Channel changes in badlands. *Geological Society of America*
769 *Bulletin*, **94**, 739-752.
- 770 Howard, A. D., Dietrich, W. E. & Seidl, M. A. 1994. Modeling fluvial erosion on regional to
771 continental scales. *Journal of Geophysical Research*, **99**, 13971-13986.
- 772 Jansen, J. D. 2006. Flood magnitude-frequency and lithologic control on bedrock river incision in
773 post-orogenic terrain. *Geomorphology*, **82**, 39-57, doi: 10.1016/j.geomorph.2005.08.018.
- 774 Jones, O. T. 1924. Longitudinal profiles of the Upper Towy drainage system. *Quarterly Journal of*
775 *the Geological Society*, **80**, 568-609.
- 776 Kirby, E., Whipple, K. X., Tang, W. & Chen, Z. 2003 Distribution of active rock uplift along the
777 eastern margin of the Tibetan Plateau: inferences from bedrock channel longitudinal long
778 profiles. *Journal of Geophysical Research*, **108**, 2217, doi: 10.1029/2001JB000861.
- 779 Kobor, J. S. & Roering, J. J. 2004. Systematic variation of bedrock channel gradients in the
780 central Oregon Coast Range: implications for rock uplift and shallow landsliding.
781 *Geomorphology*, **62**, 239-256.
- 782 Kooi, H. & Beaumont, C. 1994. Escarpment evolution on high-elevation rifted margins: Insights
783 derived from a surface process model that combines diffusion, advection, and reaction. *Journal*
784 *of Geophysical Research*, **99**, 12191-12209.
- 785 Matmon, A., Bierman, P. & Enzel, Y. 2002. Pattern and tempo of great escarpment erosion.
786 *Geology*, **30**, 1135-1138.
- 787 Merritts, D. J., Vincent, K. R. & Wohl, E. E. 1994. Long river profiles, tectonism, and eustasy: A
788 guide to interpreting fluvial terraces. *Journal of Geophysical Research*, **99**, 14031-14050.
- 789 Moore, M. W., Gleadow, A. J. W. & Lovering, J. F. 1986. Thermal evolution of rifted continental
790 margins: new evidence from fission tracks in basement apatites from southeastern Australia.
791 *Earth and Planetary Science Letters*, **78**, 255-270.

- 792 O'Brien, P. E. & Burne, R. V. 1994. The Great Cumbung Swamp - terminus of the low gradient
793 Lachlan River, Eastern Australia. *AGSO Journal of Australian Geology and Geophysics*, **15**,
794 223-233.
- 795 Ollier, C. D. & Pain, C. F. 1994. Landscape evolution and tectonics in southeastern Australia.
796 *AGSO Journal of Australian Geology and Geophysics*, **15**, 335-345.
- 797 O'Sullivan, P. B., Kohn, B. P., Foster, D. A. & Gleadow, A. J. W. 1995. Fission track data from
798 the Bathurst Batholith: evidence for rapid mid-Cretaceous uplift and erosion within the
799 eastern highlands of Australia. *Australian Journal of Earth Science*, **42**, 597-607.
- 800 O'Sullivan, P. B., Foster, D. A., Kohn, B. P. & Gleadow, A. J. W. 1996. Tectonic implications of
801 early Triassic and middle Cretaceous denudation in the eastern Lachlan Fold Belt, NSW,
802 Australia. *Geology*, **24**, 563-566.
- 803 Pazzaglia, F. J. & Gardner, T. W. 1994. Late Cenozoic flexural deformation of the middle U.S.
804 passive margin. *Journal of Geophysical Research*, **99**, 12143-12157.
- 805 Pazzaglia, F. J. & Gardner, T. W. 2000. Late Cenozoic landscape evolution of the US Atlantic
806 passive margin: insights into a North American Great Escarpment. *In*: Summerfield, M. A.
807 (ed.) *Geomorphology and Global Tectonics*. John Wiley, Chichester, 283-302.
- 808 Persano, C., Stuart, F. M., Bishop, P. & Barfod, D. 2002. Apatite (U-Th)/He age constraints on
809 the development of the Great Escarpment on the southeastern Australian passive margin.
810 *Earth and Planetary Science Letters*, **200**, 79-90.
- 811 Persano, C., Stuart, F. M., Bishop, P. & Dempster, T. 2005. Deciphering continental breakup in
812 eastern Australia by combining apatite (U-Th)/He and fission track thermochronometers.
813 *Journal of Geophysical Research*, **110**, B12405, doi: 10.1029/2004JB003325.
- 814 Reusser, L., Bierman, P., Pavich, M., Larsen, J. & Finkel, R. 2006. An episode of rapid bedrock
815 channel incision during the last glacial cycle, measured with ¹⁰Be. *American Journal of*
816 *Science*, **306**, 69-102.
- 817 Roe, G. H., Montgomery, D. R. & Hallet, B. 2002. Effects of orographic precipitation on the
818 concavity of steady-state river profiles. *Geology*, **30**, 143-146.
- 819 Sklar, L. & Dietrich, W. E. 1998. River longitudinal profiles and bedrock incision models: stream
820 power and the influence of sediment supply. *In*: Tinkler, K. J. & Wohl, E. E. (eds) *Rivers over*
821 *Rock: Fluvial Processes in Bedrock Channels*. American Geophysical Union, Geophysical
822 Monograph, **107**, 237-260.
- 823 Sklar, L. & Dietrich, W. E. 2001. Sediment supply, grain size and rock strength controls on rates
824 of river incision into bedrock. *Geology*, **29**, 1087-1090.
- 825 Stock, J. & Dietrich, W. E. 2003. Valley incision by debris flows: Evidence of a topographic
826 signature. *Water Resources Research*, **39**, 1089, doi: 10.1029/2001WR001057.
- 827 Stock, J. & Montgomery, D. R. 1999. Geologic constraints on bedrock river incision using the
828 stream power law. *Journal of Geophysical Research*, **104**, 4983-4993.

- 829 Thornbury, W. D. 1969. *Principles of Geomorphology*, 2nd edition, John Wiley, New York.
- 830 Tinkler, K. J. & Wohl, E. E. (eds). 1998. *Rivers over Rock: Fluvial Processes in Bedrock*
831 *Channels*. American Geophysical Union, Geophysical Monograph, **107**.
- 832 Tomkins, K. M. & Hesse, P. P. 2004. Evidence of Late Cenozoic uplift and climate change in the
833 stratigraphy of the Macquarie River valley, New South Wales. *Australian Journal of Earth*
834 *Sciences*, **51**, 273-290.
- 835 Tucker, G. E. & Slingerland, R. L. 1994. Erosional dynamics, flexural isostasy, and long-lived
836 escarpments: A numerical modeling study. *Journal of Geophysical Research*, **99**, 12229-
837 12243.
- 838 Tucker, G. E. & Whipple, K. X. 2002. Topographic outcomes predicted by stream erosion
839 models: sensitivity analysis and intermodel comparison. *Journal of Geophysical Research*,
840 **107**, B2, doi: 10.1029/2000JB000044.
- 841 Turowski, J. M., Lague, D. & Hovius, N. 2007. Cover effect in bedrock abrasion: A new derivation
842 and its implications for the modeling of bedrock channel morphology. *Journal of Geophysical*
843 *Research*, **112**, F04006, doi:10.1029/2006JF000697.
- 844 Twidale, C. R. 1976. On the survival of palaeoforms. *American Journal of Science*, **276**, 77-94.
- 845 Twidale, C. R. 1991. A model of landscape evolution involving increased and increasing relief
846 amplitude. *Zeitschrift für Geomorphologie*, **35**, 85-109.
- 847 Twidale, C. R. 1998. Antiquity of landforms: an 'extremely unlikely' concept vindicated. *Australian*
848 *Journal of Earth Sciences*, **45**, 657-668.
- 849 van der Beek, P., Andriessen, P. & Cloetingh, S. 1995. Morphotectonic evolution of continental
850 rifted margins: Inferences from a coupled tectonic--surface processes model and fission track
851 thermochronology. *Tectonics*, **14**, 406-421.
- 852 van der Beek, P. & Bishop, P. 2003. Cenozoic river profile development in the Upper Lachlan
853 catchment (SE Australia) as a test of quantitative fluvial incision models. *Journal of*
854 *Geophysical Research*, **108**, 2309, doi: 10.1029/2002JB002125.
- 855 van der Beek, P. & Braun, J. 1998. Numerical modelling of landscape evolution on geological
856 time-scales: a parameter analysis and comparison with the south-eastern highlands of
857 Australia. *Basin Research*, **10**, 49-68.
- 858 van der Beek, P., Braun, J. & Lambeck, K. 1999. Post-Palaeozoic uplift history of southeastern
859 Australia revisited: results from a process-based model of landscape evolution. *Australian*
860 *Journal of Earth Sciences*, **46**, 157-172.
- 861 van der Beek, P., Pulford, A. & Braun, J. 2001. Cenozoic landscape evolution in the Blue
862 Mountains (SE Australia): Lithological and tectonic controls on rifted margin morphology.
863 *Journal of Geology*, **109**, 35-56.
- 864 Veevers, J. J. (ed.) 1984. *Phanerozoic Earth History of Australia*. Clarendon Press, Oxford.

- 865 Wellman, P. 1979a. On the Cainozoic uplift of the southeastern Australian highland. *Journal of*
866 *the Geological Society of Australia*, **26**, 1-9.
- 867 Wellman, P. 1979b. On the isostatic compensation of Australian topography. *BMR Journal of*
868 *Australian Geology and Geophysics*, **4**, 373-382.
- 869 Wellman, P. 1987. Eastern Highlands of Australia: their uplift and erosion. *BMR Journal of*
870 *Australian Geology and Geophysics*, **10**, 277-286.
- 871 Wellman, P. & McDougall, I. 1974. Potassium-argon ages on the Cainozoic volcanic rocks of
872 New South Wales, Australia. *Journal of the Geological Society of Australia*, **21**, 247-272.
- 873 Whipple, K. X., Snyder, N. P. & Dollenmayer, K. 2000. Rates and processes of bedrock incision
874 by the Upper Ukak River since the 1912 Novarupta ash flow in the Valley of Ten Thousand
875 Smokes, Alaska. *Geology*, **28**, 835-838.
- 876 Whipple, K. X. & Tucker, G. E. 1999. Dynamics of the stream-power incision model: Implications for
877 height limits of mountain ranges, landscape response timescales, and research needs. *Journal*
878 *of Geophysical Research*, **104**, 17661-17674.
- 879 Wohl, E. E. & Merritts, D. M. 2001. Bedrock channel morphology. *Geological Society of America*
880 *Bulletin*, **113**, 1205-1212.
- 881 Young, R. W. 1983. The tempo of geomorphological change: evidence from southeastern
882 Australia. *Journal of Geology*, **91**, 221-230.
- 883 Young, R. W. & McDougall, I. 1993. Long-term landscape evolution: Early Miocene and modern
884 rivers in southern New South Wales, Australia. *Journal of Geology*, **101**, 35-49.
- 885

886 Figure captions

887

888 Fig. 1. (a) Long profile of a hypothetical stream (lower line) with $\lambda = 0.9$ and $k = 50$ for all reaches
 889 and where the standard error of elevation is 2 m and normally distributed; the reach from $D =$
 890 800 to $D = 720$ is a diffuse knickpoint of 40 m fall generated by the headward propagation of a
 891 base-level fall of 40m. The plot shows the downstream projection of the equilibrium profile
 892 upstream of A in accordance with the DS model (upper line); the method of projection is
 893 presented by Goldrick & Bishop (2007). The DS-based estimate of the amount of incision in
 894 response to the 40 m base-level fall is 35 m (i.e., $H^* = 35$ m). (b) DS plot of this stream, showing
 895 the knickpoint at A.

896

897 Fig. 2. The Lachlan River's uplands (bedrock) drainage net. Box gives the area in Fig. 4.

898

899 Fig. 3. Geology of the Lachlan's uplands (bedrock) catchment. The Tertiary basaltic volcanics
 900 upstream of Cowra at the confluence of the Boorowa and Lachlan Rivers is the 12 Myr old
 901 Boorowa basalt. Box indicates the area in Fig. 4.

902

903 Fig. 4. The drainage network, geology and sub-basaltic contours of the upper Lachlan
 904 catchment. Sub-basaltic contours (20 m contour interval) have been taken from Fig. 8 of Bishop
 905 *et al.* (1985) and their elevations decrease westwards and northwards. These contour lines have
 906 not been labelled in order to avoid clutter and because it is their relative spacing and orientation
 907 rather than their absolute elevations that are important; likewise, we number (rather than name)
 908 the streams to avoid clutter and multiple stream names. The Bevendale Basalt is the southern-
 909 and western-most linear flow remnant (flowing westwards and then northwards adjacent to the
 910 Lachlan trunk stream [stream number 61]), and the Wheeo Basalt is the parallel linear flow, to
 911 the north and northeast of the Bevendale Basalt (Bishop 1984). The broad tabular basalt in the
 912 east, at the continental drainage divide, is the Divide Basalt. LGF = Lake George Fault.

913

914 Fig. 5. Detail of drainage network, geology and sub-basaltic contours in the vicinity of Streams 59
 915 and 60. The asterisk marks the western limit of the possible location of the drainage divide for
 916 the basalt-filled east-west tributary; the eastern limit for the divide location is the catchment
 917 boundary in the east (the continental drainage divide). The text gives more detail.

918

919 Fig. 6. The DS plot (top) and long profile (bottom) of Stream 59 (left) and Stream 60 (right). Solid
 920 diamonds: data points used for profile reconstruction; broken lines: upper and lower confidence
 921 limits of projections of reconstructed profiles; squares: elevations of base of basalt (from Fig. 5);
 922 thin vertical lines above squares: estimated thickness of the basalt flow; thin vertical lines below

923 squares: uncertainty of elevation for base of the basalt. Shading and two-letter labels indicate
924 underlying geology (Ad: Adaminaby Group (Palaeozoic quartz-rich metasediments); Wy:
925 Wyangala batholith (Palaeozoic granitic rocks); thick vertical line: hornfels ridge).

926

927 Fig. 7. (a) DS plot and (b) long profile of the sub-basaltic elevations of the east-west (tributary) E
928 Miocene lava flow, assuming that the Miocene divide was at the asterisk in Fig. 5.

929

930 Fig. 8. The DS plot (top) and long profile (bottom) of (a) Stream 67 and (b) Stream 68. Symbols
931 as in Fig. 6.

932

933 Fig. 9. The DS plot (top) and long profile (bottom) of (a) Stream 69 and (b) Stream 72. Symbols
934 as in Fig. 6.

935

936 Fig. 10. Schematic of hypothesised post-eruption evolution of tributaries of the upper Lachlan.
937 After the eruption, the trunk stream is re-established on the left side of its basalt-filled valley.
938 Trunk-stream incision generates knickpoints where right-bank tributaries cross the basalt; left-
939 bank tributaries do not have to incise basalt. Long-profile projections show that the right-bank
940 tributaries above the KP are graded to the base of the basalt (Fig. 6), whereas the western
941 tributaries did not have to negotiate the basalt and so do not exhibit such grading (Figs 8 and 9,
942 especially Fig. 8b). In the top three cartoons an earlier KP is also shown propagating up the
943 right-bank tributary.

944

945 Fig. 11. Numerical simulation of the evolution of the DS plot and long profile of an initially graded
946 stream profile after the emplacement of a segment of resistant lithology. The broken line on the
947 long profile is the original profile and the closely-spaced vertical lines indicate the extent and
948 thickness of the resistant lithology.

Table 1. Values of H^* for long profile projections to the trunk Lachlan River of the graded reaches upstream of the downstream-most knickpoint in the upper Lachlan's eastern (right-bank) tributaries (see Figure 4 for location of streams)

Projected stream	H^* (m) at confluence with Lachlan
(a)	
56	63 ± 4
57	16 ± 4
58	80 ± 5
59	60 ± 10
60	83 ± 13
(b)	
57 (upstream)	122
58 (upstream)	143 ± 10
Miocene trib.	103 ± 30

Table 2. Values of H^* for long profile projections of upstream graded reaches of the western (left-bank) tributaries to the upper Lachlan River; and the confluences to which they have been projected

Projected Stream	H^* (m) at confluence	Confluence
67	30 ± 2	67 & 68
68	26 ± 17	67 & 68
68	25 ± 14	68 & 69
69	16 ± 5	68 & 69
73	21 ± 0	73 & 61

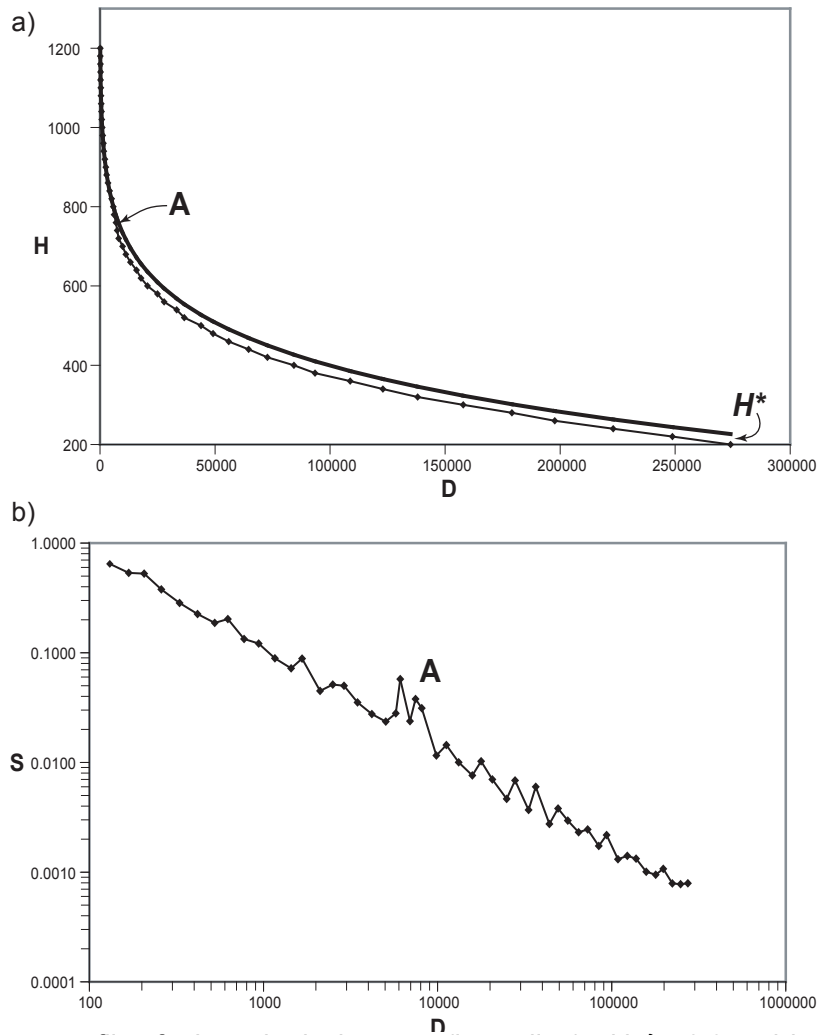
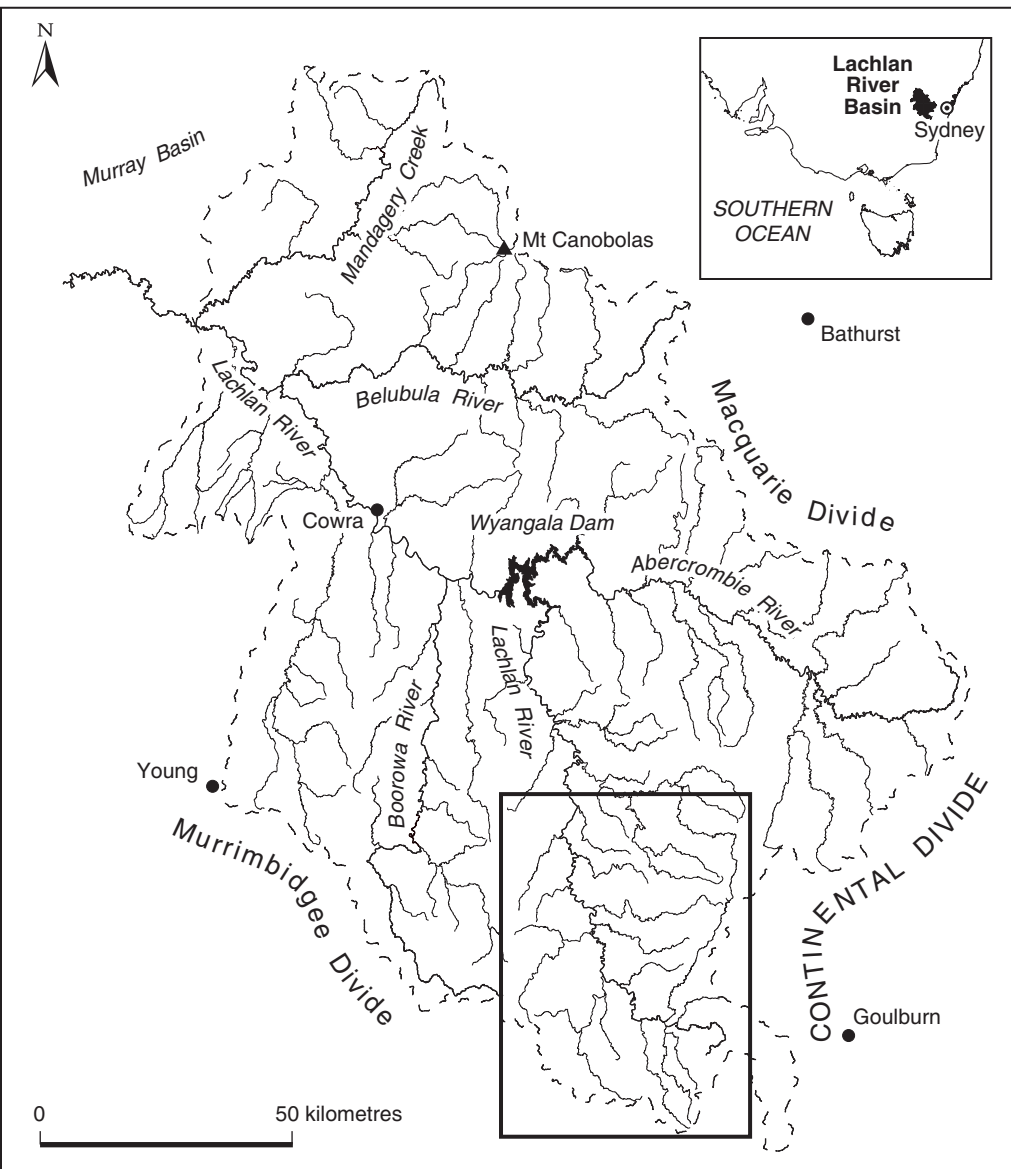


Fig. 1. (a) Long profile of a hypothetical stream (lower line) with $\lambda = 0.9$ and $k = 50$ for all reaches 889 and where the standard error of elevation is 2 m and normally distributed; the reach from $D = 890\ 800$ to $D = 720$ is a diffuse knickpoint of 40 m fall generated by the headward propagation of a 891 base-level fall of 40m. The plot shows the downstream projection of the equilibrium profile 892 upstream of A in accordance with the DS model (upper line); the method of projection is 893 presented by Goldrick & Bishop (2007). The DS-based estimate of the amount of incision in 894 response to the 40 m base-level fall is 35 m (i.e., $H^* = 35$ m). (b) DS plot of this stream, showing 895 the knickpoint at A.

Fig. 2. The Lachlan River's uplands (bedrock) drainage net. Box gives the area in Fig. 4.



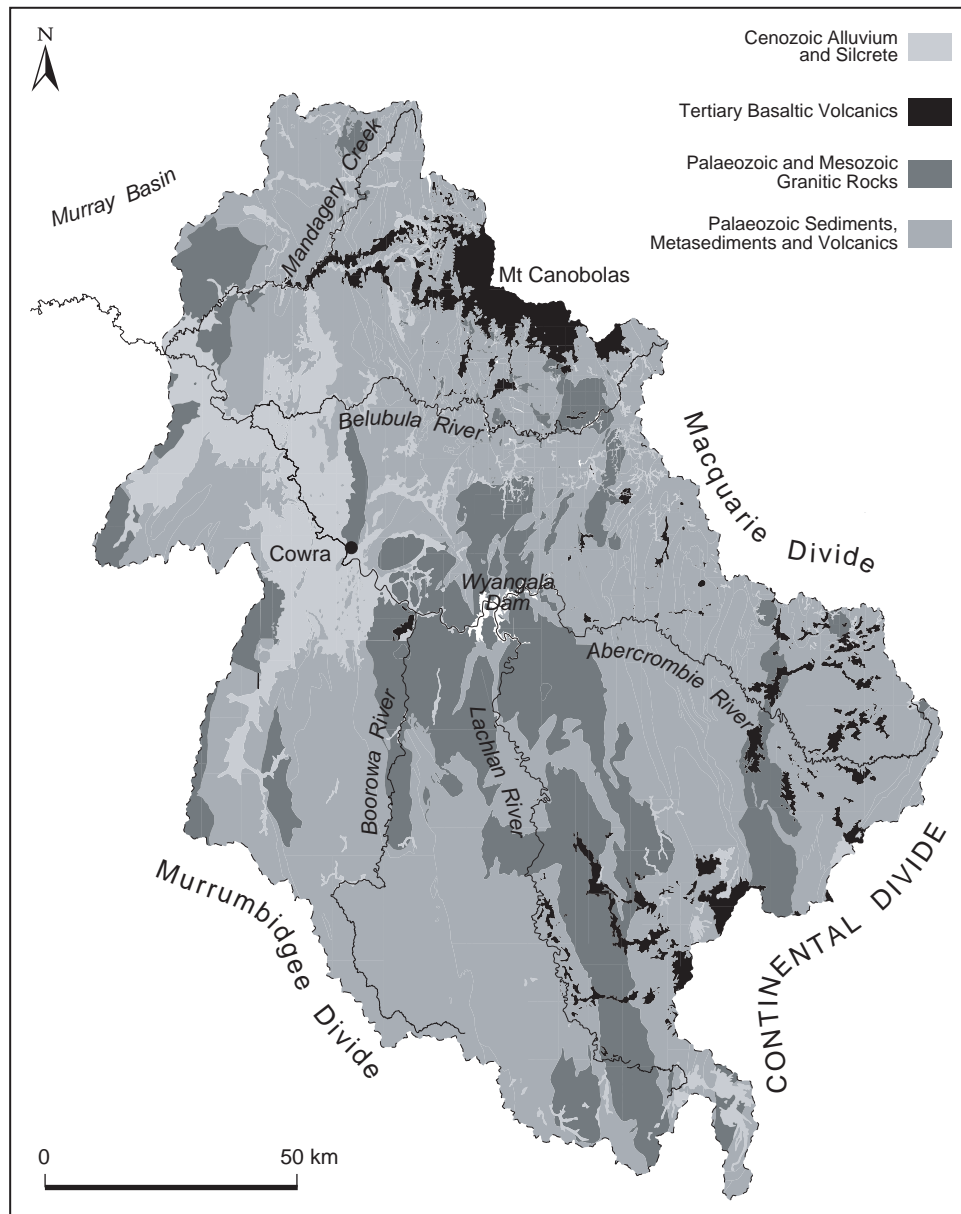


Fig. 3. Geology of the Lachlan's uplands (bedrock) catchment. The Tertiary basaltic volcanics 900 upstream of Cowra at the confluence of the Boorowa and Lachlan Rivers is the 12 Myr old 901 Boorowa basalt.

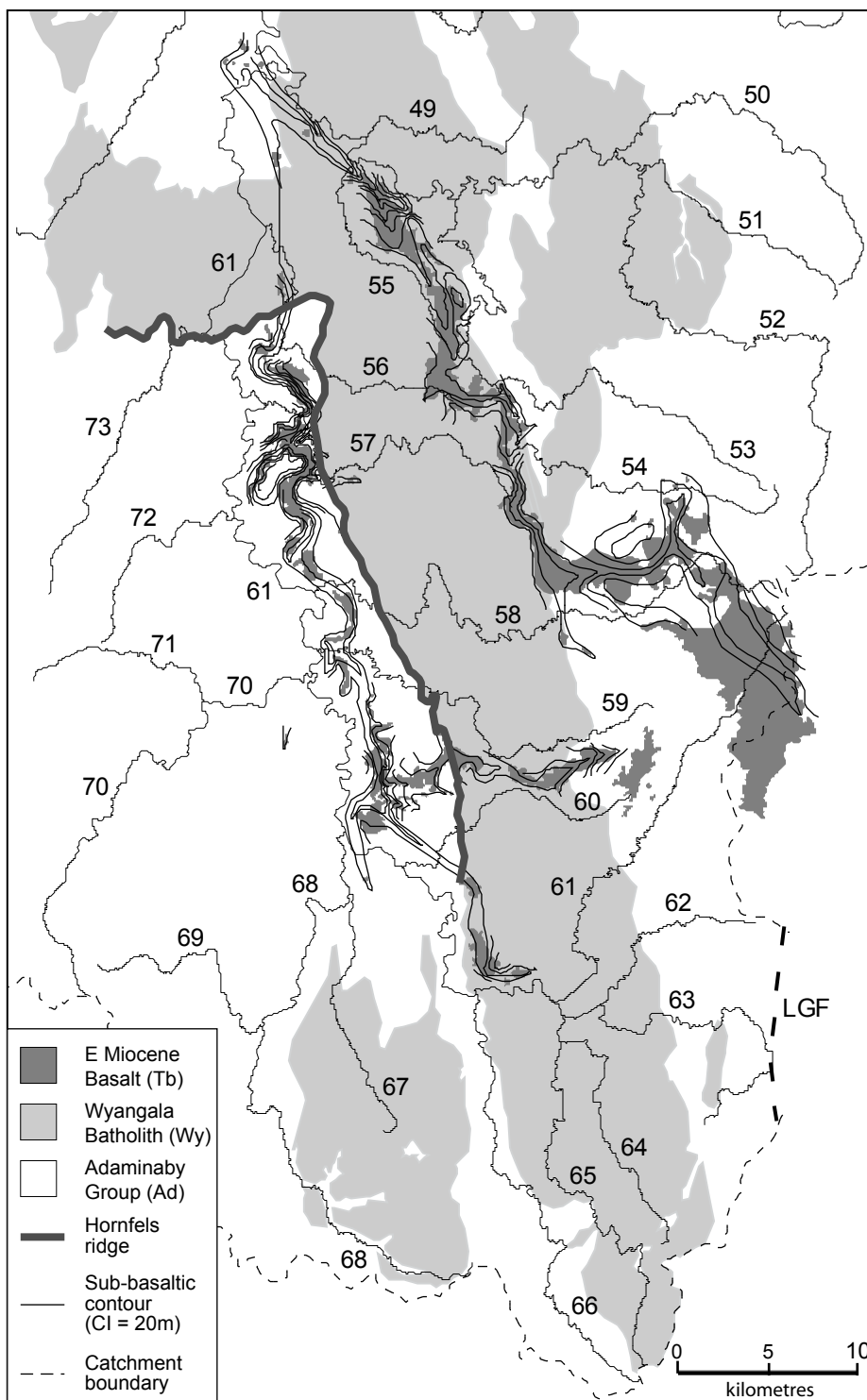


Fig. 4. The drainage network, geology and sub-basaltic contours of the upper Lachlan 904 catchment. Sub-basaltic contours (20 m contour interval) have been taken from Fig. 8 of Bishop 905 *et al.* (1985) and their elevations decrease westwards and northwards. These contour lines have 906 not been labelled in order to avoid clutter and because it is their relative spacing and orientation 907 rather than their absolute elevations that are important; likewise, we number (rather than name) 908 the streams to avoid clutter and multiple stream names. The Bevendale Basalt is the southern 909 and western-most linear flow remnant (flowing westwards and then northwards adjacent to the 910 Lachlan trunk stream [stream number 61]), and the Wheeo Basalt is the parallel linear flow, to 911 the north and northeast of the Bevendale Basalt (Bishop 1984). The broad tabular basalt in the 912 east, at the continental drainage divide, is the Divide Basalt. LGF = Lake George Fault.

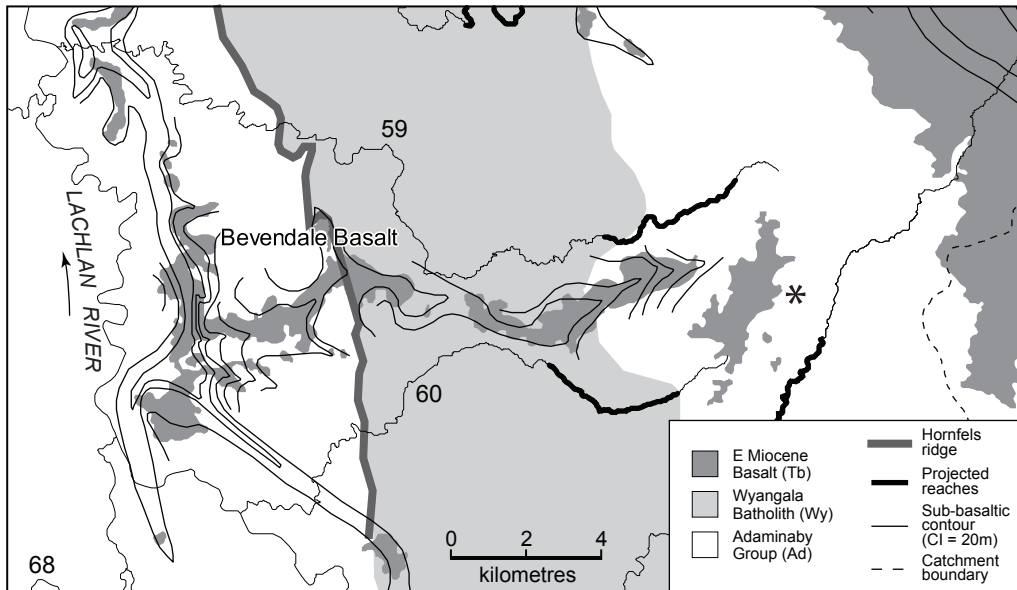


Fig. 5. Detail of drainage network, geology and sub-basaltic contours in the vicinity of Streams 59 915 and 60. The asterisk marks the western limit of the possible location of the drainage divide for 916 the basalt-filled east-west tributary; the eastern limit for the divide location is the catchment 917 boundary in the east (the continental drainage divide). The text gives more detail.

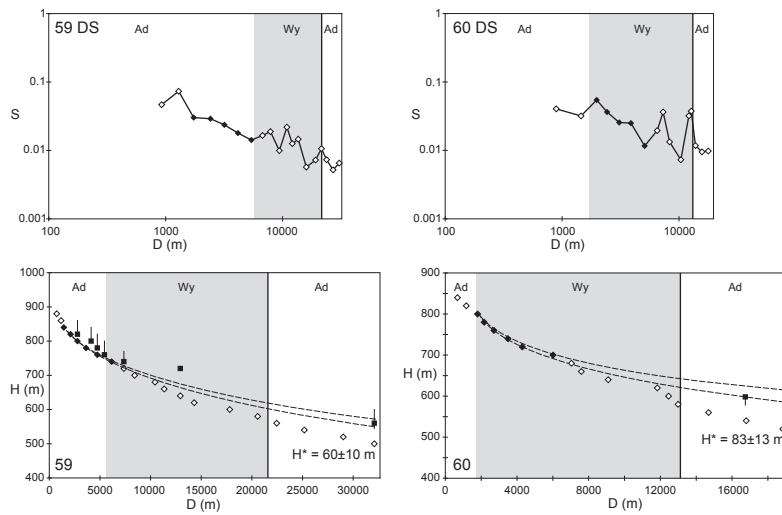


Fig. 6. The DS plot (top) and long profile (bottom) of Stream 59 (left) and Stream 60 (right). Solid 920 diamonds: data points used for profile reconstruction; broken lines: upper and lower confidence 921 limits of projections of reconstructed profiles; squares: elevations of base of basalt (from Fig. 5); 922 thin vertical lines above squares: estimated thickness of the basalt flow; thin vertical lines below squares: uncertainty of elevation for base of the 923 basalt. Shading and two-letter labels indicate 924 underlying geology (Ad: Aaminaby Group (Palaeozoic quartz-rich metasediments); Wy: 925 Wyangala batholith (Palaeozoic granitic rocks); thick vertical line: hornfels ridge).

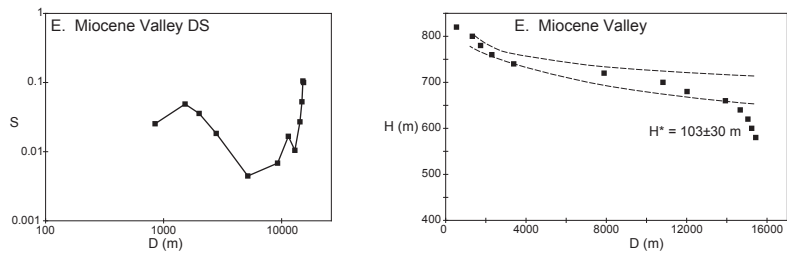


Fig. 7. (a) DS plot and (b) long profile of the sub-basaltic elevations of the east-west (tributary) E 928 Miocene lava flow, assuming that the Miocene divide was at the asterisk in Fig. 5.

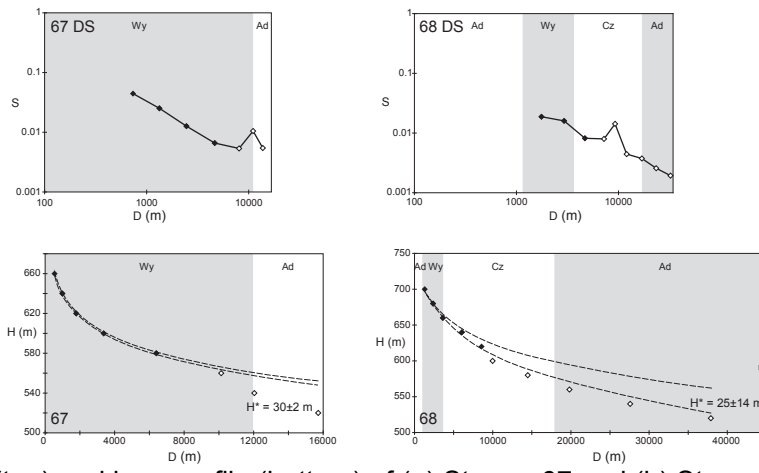


Fig. 8. The DS plot (top) and long profile (bottom) of (a) Stream 67 and (b) Stream 68. Symbols 931 as in Fig. 6.

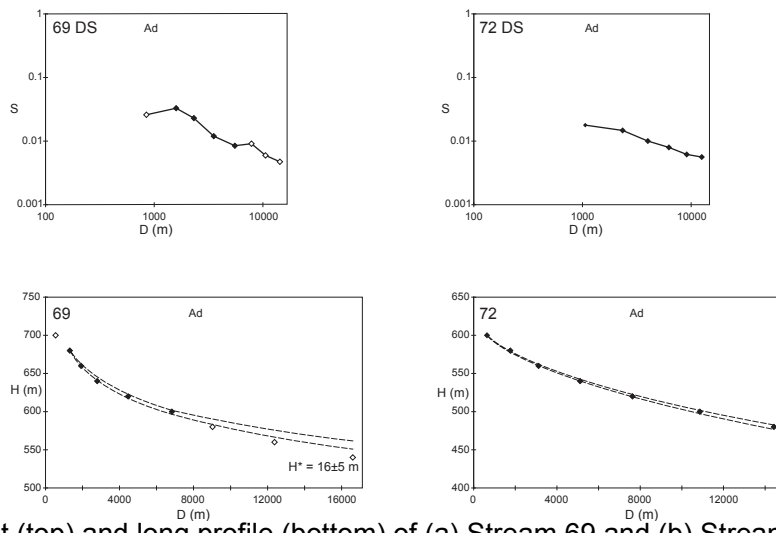


Fig. 9. The DS plot (top) and long profile (bottom) of (a) Stream 69 and (b) Stream 72. Symbols 934 as in Fig. 6.

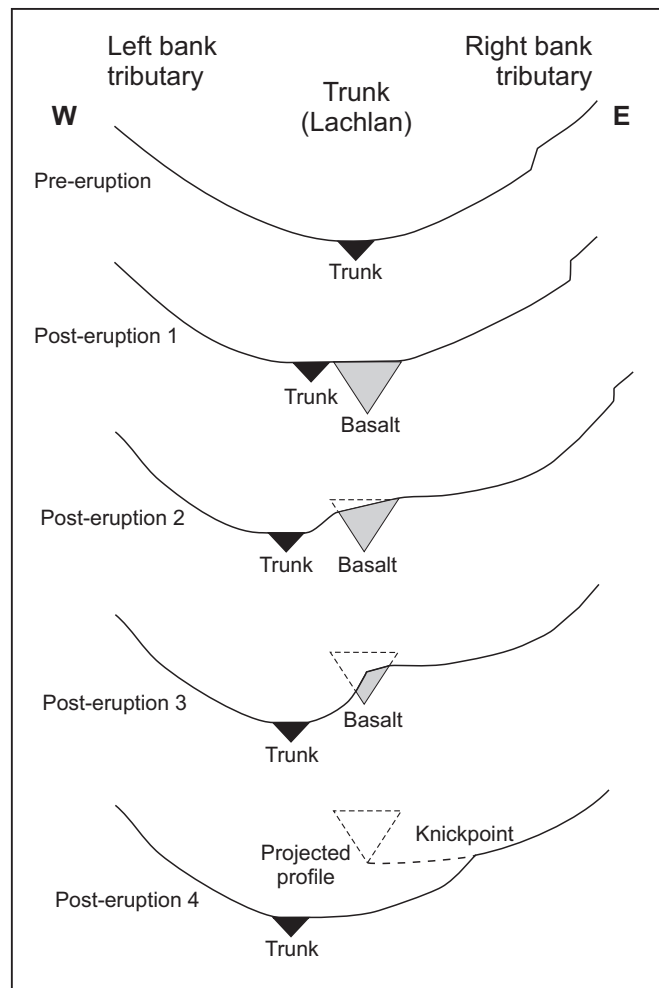


Fig. 10. Schematic of hypothesised post-eruption evolution of tributaries of the upper Lachlan.
 937 After the eruption, the trunk stream is re-established on the left side of its basalt-filled valley.
 938 Trunk-stream incision generates knickpoints where right-bank tributaries cross the basalt; left
 939 bank tributaries do not have to incise basalt. Long-profile projections show that the right-bank
 940 tributaries above the KP are graded to the base of the basalt (Fig. 6), whereas the western
 941 tributaries did not have to negotiate the basalt and so do not exhibit such grading (Figs 8 and 9,
 942 especially Fig. 8b). In the top three cartoons an earlier KP is also shown propagating up the
 943 right-bank tributary.

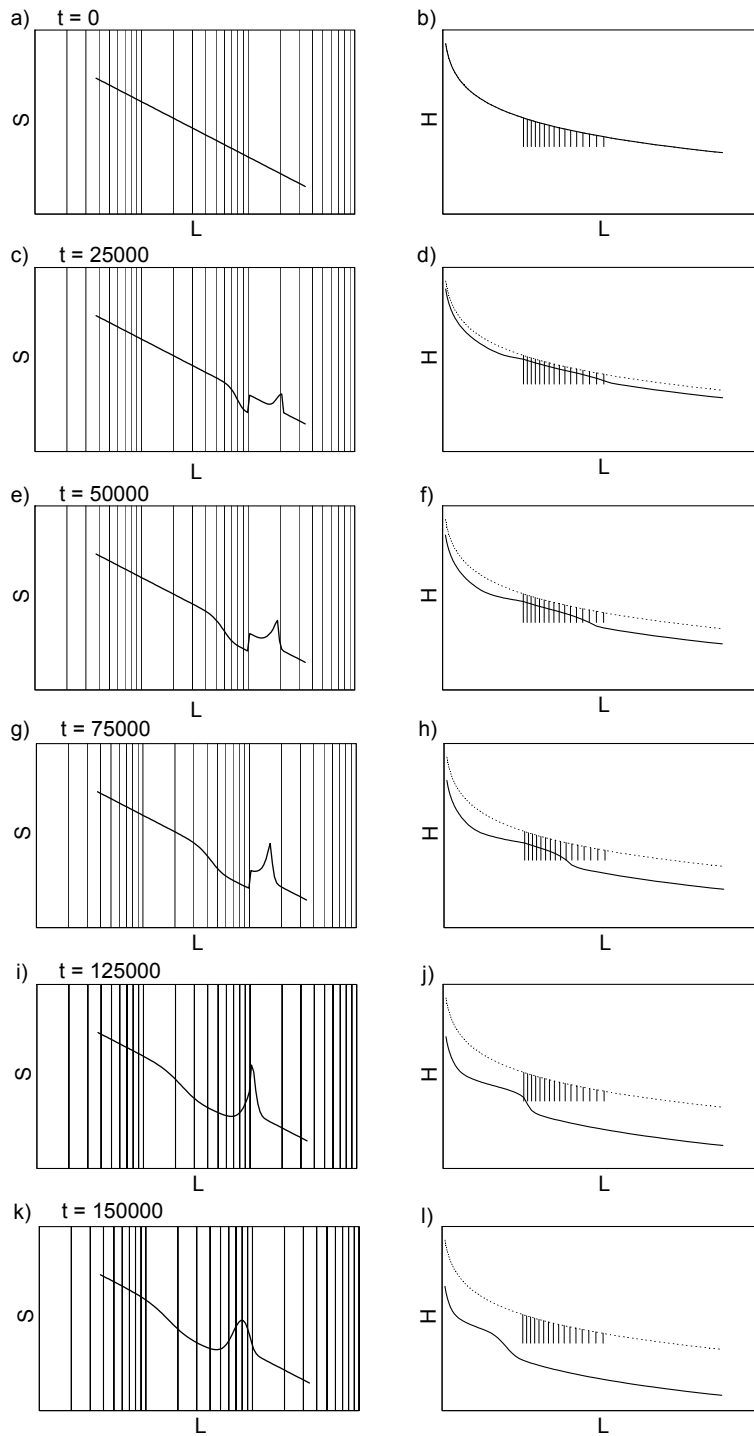


Fig. 11. Numerical simulation of the evolution of the DS plot and long profile of an initially graded 946 stream profile after the emplacement of a segment of resistant lithology. The broken line on the 947 long profile is the original profile and the closely-spaced vertical lines indicate the extent and 948 thickness of the resistant lithology.